Unique Complexation of 1,4-Diaza-1,3-butadiene Ligand on Half-Metallocene Fragments of Niobium and Tantalum

Kazushi Mashima,* Yutaka Matsuo, and Kazuhide Tani*

Department of Chemistry, Graduate School of Engineering Science, Osaka University, Toyonaka, Osaka 560-8531, Japan

Received December 8, 1998

We report the synthesis of half-metallocene 1,4-diaza-1,3-butadiene (dad) complexes of niobium and tantalum and the flexible coordination modes of the dad ligand. Treatment of $MCl_4(\eta^5\text{-}C_5R_5)$ (**1a**, M = Ta, R = CH_3; **1b**, M = Ta, R = H; **2a**, M = Nb, R = CH_3; **2b**, M = Nb, R = H) with 1 equiv of a dilithium salt of 1,4-bis(*p*-methoxyphenyl)-1,4-diaza-1,3-butadiene (*p*-$MeOC_6H_4$-dad) in THF yielded the corresponding half-sandwich 1,4-diaza-1,3-butadiene complexes $MCl_2(\eta^5\text{-}C_5R_5)(\eta^4\text{-}supine\text{-}p\text{-}MeOC_6H_4\text{-dad})$ (**3a**, M = Ta, R = CH_3; **3b**, M = Ta, R = H; **4a**, M = Nb, R = CH_3; **4b**, M = Nb, R = H). Similar reaction of **1a** with the dianions of 1,4-bis(*p*-tolyl)-1,4-diaza-1,3-butadiene (*p*-Tol-dad), 1,4-bis(*o*-tolyl)-1,4-diaza-1,3-butadiene (*o*-Tol-dad), and 1,4-dicyclohexyl-1,4-diaza-1,3-butadiene (Cy-dad) afforded tantalum complexes $TaCl_2Cp^*(\eta^4\text{-}supine\text{-}p\text{-Tol-dad})$ (**5**) (Cp* = pentamethylcyclopentadienyl), $TaCl_2Cp^*(\eta^4\text{-}supine\text{-}o\text{-Tol-dad})$ (**6**), and $TaCl_2Cp^*(\eta^4\text{-}supine\text{-Cy-dad})$ (**7**), respectively. When a dinuclear Ta(III) complex $[TaCl_2Cp^*]_2$ (**8**) was treated with 1,4-bis(2,6-diisopropylphenyl)-1,4-diaza-1,3-butadiene ($(^i\text{Pr})_2C_6H_3$-dad), a $\eta^2\text{-}C,N$-imine complex $TaCl_2Cp^*(\eta^2\text{-}C,N\text{-}(^i\text{Pr})_2C_6H_3\text{-dad})$ (**9**) was formed. Dialkylation of the dichloro complexes caused the change of the orientation of the dad ligand from *supine* fashion to a *prone* one of dimethyl complexes $TaMe_2Cp^*(\eta^4\text{-}prone\text{-dad})$ (**10**, dad = *p*-$MeOC_6H_4$-dad; **11**, dad = *o*-Tol-dad) and bis(benzyl) complexes $M(CH_2Ph)_2Cp^*(\eta^4\text{-}prone\text{-dad})$ (**12**, M = Ta, dad = *p*-$MeOC_6H_4$-dad; **13**, M = Nb, dad = *p*-$MeOC_6H_4$-dad; **14**, M = Ta, dad = Cy-dad), while a mono(benzyl) complex $Ta(CH_2Ph)ClCp^*(\eta^4\text{-}supine\text{-}o\text{-Tol-dad})$ (**16**) kept the *supine* orientation. The bis(benzyl) complexes **12**−**14** thus isolated were thermally stable in solid state, but in solution these complexes gradually decomposed to give the corresponding benzylidene complexes $M(=CHPh)Cp^*(\eta^4\text{-}prone\text{-dad})$ (**17**, M = Ta, dad = *p*-$MeOC_6H_4$-dad; **18**, M = Nb, dad = *p*-$MeOC_6H_4$-dad; **19**, M = Ta, dad = Cy-dad) with the release of toluene. Treatments of **3a**,**b**, **4a**,**b**, **5**, and **7** with a slight excess of 1,3-butadiene−magnesium adduct afforded mixed-ligand 16-electron complexes $M(\eta^5\text{-}C_5R_5)(\eta^2\text{-}N,N'\text{-}p\text{-}MeOC_6H_4\text{-dad})(\eta^4\text{-}s\text{-}cis\text{-}1,3\text{-butadiene})$ (**20a**, M = Ta, R = CH_3; **20b**, M = Ta, R = H; **21a**, M = Nb, R = CH_3; **21b**, M = Nb, R = H) and $TaCp^*(\eta^2\text{-}N,N'\text{-dad})(\eta^4\text{-}s\text{-}cis\text{-}1,3\text{-butadiene})$ (**22**, dad = *p*-Tol-dad; **23**, dad = Cy-dad), respectively. These complexes showed characteristic intense red or purple color due to LMCT bands where the filled N(pπ) orbital is donated to the empty M(dπ*) orbital.

Introduction

Recent development in the metallocene chemistry of early transition metals is due to their potential applicability as catalysts of various organic reactions as well as polymerization and as source of versatile materials.[1,2] To attain legitimate metallocene complexes for each purpose, modification of the cyclopentadienyl ligand, including the *ansa*-type bis(cyclopentadienyl) ligand, has been extensively investigated. Another, more flexible approach may be a half-metallocene system, in which one Cp ligand of the metallocene is replaced by different kinds of ancillary ligand. We have chosen diene as a ligand for the half-metallocene complexes of niobium and tantalum; the diene complexes having "$M(\eta^5\text{-}C_5R_5)$(1,3-diene)" fragments are isoelectronic and isolobal to group 4 metallocene fragments "MCp_2", which are 14-electron species. We had found not only that these metallocene-like fragments stabilized various reactive species such as benzyne[3] similar to the corresponding metallocene complexes of group 4 metals but also that *cis*-dialkyl derivatives were catalyst precursors for the living polymerization of ethylene[4−6] and the stereoselective ROMP of norbornene.[7−9]

(1) Metallocenes: Togni, A., Halterman, R. L., Eds.; Wiley-VCH: Weinheim, Germany, 1998; Vol. 1 and 2.
(2) Mashima, K.; Nakayama, Y.; Nakamura, A. *Adv. Polym. Sci.* **1997**, *133*, 1.
(3) Mashima, K.; Tanaka, Y.; Nakamura, A. *Organometallics* **1995**, *14*, 5642.
(4) Mashima, K.; Fujikawa, S.; Tanaka, Y.; Urata, Y.; Oshiki, T.; Tanaka, E.; Nakamura, A. *Organometallics* **1995**, *14*, 2633.
(5) Mashima, K.; Fujikawa, S.; Urata, H.; Tanaka, E.; Nakamura, A. *J. Chem. Soc., Chem. Commun.* **1994**, 1623.
(6) Mashima, K.; Fujikawa, S.; Nakamura, A. *J. Am. Chem. Soc.* **1993**, *115*, 10990.

10.1021/om981003b CCC: $18.00
Publication on Web 03/19/1999

Chart 1

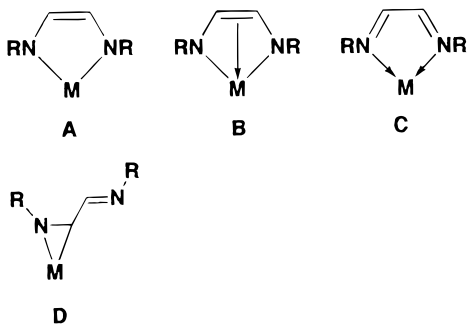

Herein we report the syntheses of various 1,4-diaza-1,3-butadiene (dad) complexes of niobium and tantalum. The dad ligand is known to exhibit the unique coordination feature of binding to the metal center in several modes, *N*,*N*′-chelation (A, B, and C) and η^2-*C*,*N*-imine (D) (Chart 1).[10,11] By tuning the substituents on the dad ligand and on the metal center, the niobium and tantalum complexes having three coordination modes, A, B, and D, have been prepared, although the mode C has been reported for many late transition metal complexes. Furthermore, since these are the half-metallocene complexes, the σ^2,π-endiamido ligand (mode B) can adopt two conformations, i.e., *supine* and *prone*, relative to the η^5-C_5R_5 ligand, depending sensitively on the coordination environment on the metal center. A part of this work was the subject of preliminary communications,[12] and the syntheses of closely related tantalum complexes have recently been reported.[13,14]

Results and Discussion

Synthesis and Characterization of Dichloro Complexes of Niobium and Tantalum Bearing a dad Ligand. Treatment of tetrachloro compounds of tantalum and niobium, $MCl_4(\eta^5$-$C_5R_5)$ (**1a**, M = Ta, R = CH_3; **1b**, M = Ta, R = H; **2a**, M = Nb, R = CH_3; **2b**, M = Nb, R = H), with a dilithium salt[15] of 1,4-bis(*p*-methoxyphenyl)-1,4-diaza-1,3-butadiene (*p*-$MeOC_6H_4$-dad) in THF led to the formation of the corresponding half-sandwich 1,4-diaza-1,3-butadiene complexes, $MCl_2(\eta^5$-$C_5R_5)(\eta^4$-*supine*-*p*-$MeOC_6H_4$-dad) (**3a**, M = Ta, R = CH_3; **3b**, M = Ta, R = H; **4a**, M = Nb, R = CH_3; **4b**, M = Nb, R = H), whose formulations were in accordance with spectroscopic data and combustion analyses. These tantalum and niobium complexes were obtained as yellow and red precipitates, respectively. These were stable in the solid state, but gradually decomposed in solution upon exposure to air. The inner $H^{2,3}$ protons of the *p*-$MeOC_6H_4$-dad ligand were observed as a singlet in the olefinic region (δ 6.00 for **3a**; δ 6.09 for **3b**; δ 6.05 for **4a**; δ 6.19 for **4b**), suggesting a distinct σ^2,π-endiamido structure (mode B in Chart 1). Furthermore, for half-metallocene complexes, two conformations, i.e., *supine* and *prone*, of the dad ligand in the direction of the cyclopentadienyl ligand are possible. On the basis of NMR spectral data compared with those of the *prone* complexes (vide infra), we concluded that the dad ligand of **3** and **4** predominantly adopted the *supine* conformation, which was further confirmed by X-ray crystallographic studies (vide infra).

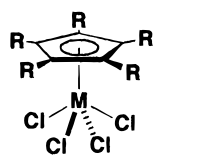

1a: M = Ta; R = CH_3
1b: M = Ta; R = H
2a: M = Nb; R = CH_3
2b: M = Nb; R = H

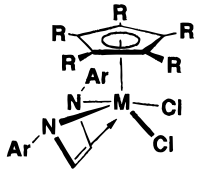

3a: M = Ta; R = CH_3
3b: M = Ta; R = H
4a: M = Nb; R = CH_3
4b: M = Nb; R = H

Ar = *p*-MeO-C_6H_4

In the case of the other *p*-substituted dad ligand, 1,4-bis(*p*-tolyl)-1,4-diaza-1,3-butadiene (*p*-Tol-dad), we also obtained $TaCl_2Cp^*(\eta^4$-*supine*-*p*-Tol-dad) (**5**) (Cp* = pentamethylcyclopentadienyl) in modest yield after treating **1a** with the corresponding dad lithium salt in THF. In contrast, the bulkiness due to the ortho-substituted phenyl group of the dad ligand affected the complexation with half-metallocene fragments of niobium and tantalum. The reactions of **1a** with dilithium salts of 1,4-bis(2,6-dimethylphenyl)-1,4-diaza-1,3-butadiene (Xyl-dad) and 1,4-bis(2,6-diisopropylphenyl)-1,4-diaza-1,3-butadiene [$(^i$Pr$)_2C_6H_3$-dad] resulted in the complicated mixture, from which, in both reactions, any identifiable products could not be obtained. On the other hand, the reaction of **1a** with a dilithium salt of 1,4-bis(*o*-tolyl)-1,4-diaza-1,3-butadiene (*o*-Tol-dad) afforded the corresponding tantalum complex, $TaCl_2Cp^*(\eta^4$-*supine*-*o*-Tol-dad) (**6**). Cyclohexyl substitutions on nitrogen atoms afforded $TaCl_2Cp^*(\eta^4$-*supine*-Cy-dad) (**7**) on treating **1a** with a dilithium salt of the 1,4-dicyclohexyl-1,4-diaza-1,3-butadiene (Cy-dad) in a similar manner.

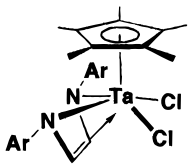

5: Ar = *p*-Tolyl
6: Ar = *o*-Tolyl

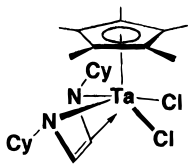

7

Another synthetic method starting from a dinuclear Ta(III) complex, $[TaCl_2Cp^*]_2$ (**8**), can be applicable to the preparation of the dad complexes.[16,17] When the benzene solution of **8** was treated with 1 equiv of *p*-$MeOC_6H_4$-dad, the deep green color of **8** faded out and the yellow complex **3a** was formed in quantitative yield, monitored by the ^{1}H NMR spectrum. Reaction of **8** with *o*-Tol-dad afforded the complex **6**, while reaction with

(7) Mashima, K.; Tanaka, Y.; Kaidzu, M.; Nakamura, A. *Organometallics* **1996**, *15*, 2431.
(8) Mashima, K.; Kaidzu, M.; Nakayama, Y.; Nakamura, A. *Organometallics* **1997**, *16*, 1345.
(9) Mashima, K.; Kaidzu, M.; Tanaka, Y.; Nakayama, Y.; Nakamura, A.; Hamilton, J. G.; Rooney, J. J. *Organometallics* **1998**, *17*, 4183.
(10) van Koten, G.; Vrieze, K. *Adv. Organomet. Chem.* **1982**, *21*, 151.
(11) Vrieze, K. *J. Organomet. Chem.* **1986**, *300*, 307.
(12) Mashima, K.; Matsuo, Y.; Tani, K. *Chem. Lett.* **1997**, 767.
(13) Pindado, G. J.; Thornton-Pett, M.; Bochmann, M. *J. Chem. Soc., Dalton Trans.* **1998**, 393.
(14) Kawaguchi, H.; Yamamoto, Y.; Asaoka, K.; Tatsumi, K. *Organometallics* **1998**, *17*, 4380.
(15) Scholz, J.; Richter, B.; Goddard, R.; Krüger, C. *Chem. Ber.* **1993**, *126*, 57.
(16) Ting, C.; Baenzinger, N. C.; Messerle, L. *J. Chem. Soc., Chem. Commun.* **1988**, 1133.
(17) Messerle, L. *Chem. Rev.* **1988**, *88*, 1229.

Xyl-dad did not give any identifiable product, consistent with the attempted synthesis by metathesis reaction. On the other hand, treatment of **8** with (^{i}Pr)$_2$C$_6$H$_3$-dad resulted in the unique formation of an orange complex TaCl$_2$Cp*(η^2-*C,N*-(^{i}Pr)$_2$C$_6$H$_3$-dad) (**9**), in which the dad ligand coordinated to the tantalum center in η^2-*C,N*-imine coordination (mode D). Such a η^2-*C,N*-coordination of the dad ligand has already been reported for a niobium complex, [Nb(η^4-^{t}Bu-dad)(η^2-*C,N*-^{t}Bu-dad)]$_2$(μ-^{t}Bu-dad) (^{t}Bu-dad = 1,4-di(*tert*-butyl)-1,4-diaza-1,3-butadiene),[18] and a tantalum complex, Ta(S^{t}Bu)$_2$Cp*(η^2-*C,N*-^{t}Bu-dad).[14] The complex **9** decomposed upon exposure to air or during the attempted isolation. The ^{1}H NMR spectrum of **9** displayed the asymmetric signals due to the presence of an asymmetric carbon center bound to the tantalum atom; the H^2 proton appeared at higher field (δ 3.67) than that (δ 7.73) of the other imine H^3 proton, indicating that one of the two C=N moieties coordinated to the tantalum atom in an azametallacyclopropane structure,[19−21] while the other was free from coordination.

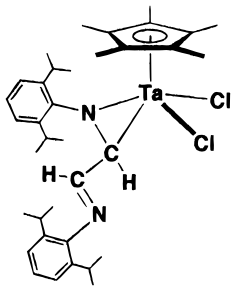

9

Crystal Structures of Dichloro Complexes of Niobium and Tantalum, 3a,b, 4a, 5, and 7. The molecular structures of the complexes **3a**, **3b**,[12] **4a**, **5**, and **7** were determined by X-ray crystallographic studies. Figure 1 shows the molecular structures of **3a** and **4a**. Selected bond distances and angles of all these complexes are listed in Table 1. Although **4a** is a niobium complex and others are tantalum complexes with different combinations of η^5-C$_5$R$_5$ and dad ligands, they are essentially isomorphous. Each complex adopts a four-legged piano stool geometry comprised of a η^5-C$_5$R$_5$ ligand, two chlorine atoms, and a dad ligand; this geometry is similar to that of NbCl$_2$Cp(η^4-*supine*-^{t}Bu-dad)[22] and TaCl$_2$Cp*(η^4-*supine*-^{i}Pr-dad) (^{i}Pr-dad = 1,4-di(isopropyl)-1,4-diaza-1,3-butadiene).[14] Noteworthy is that the dad ligand is coordinated to the metal in the *supine* σ^2,π-enediamide structure (mode B in Chart 1). The canonical structure B corresponds to the tendency that the 1,3-butadiene bound to the tantalum center has a contribution of a metallacyclopentene structure, and in addition, three C−C bond distances of the diene ligand are sequentially long−short−long.[23] Although such a long−short−long alternation is not clearly observed for the dad ligand, the C^1−C^2 distance of the dad ligand is significantly shortened compared with that of a free ligand, *s-trans*-Cy-dad (1.457(2) Å),[10] and the

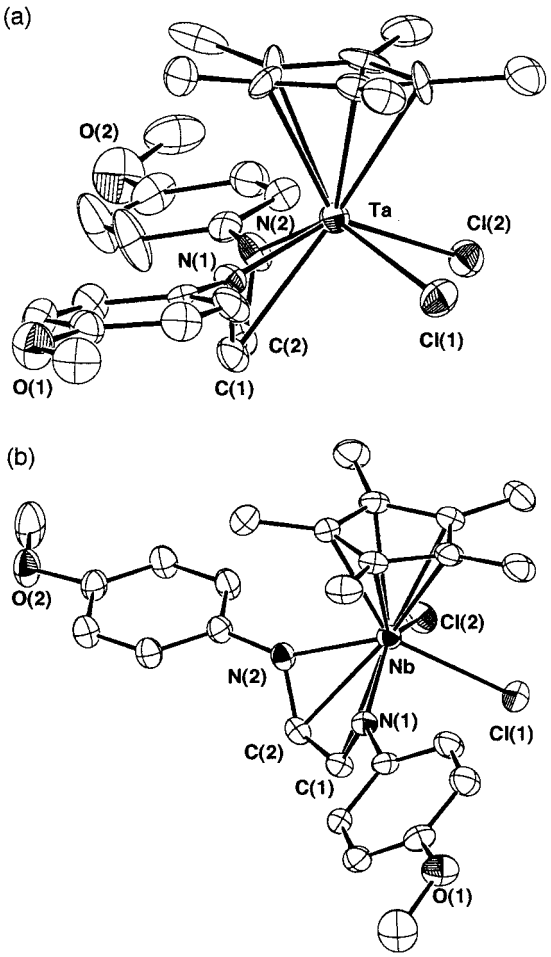

Figure 1. (a) Molecular structure of **3a** with the labeling scheme. (b) Molecular structure of **4a** with the labeling scheme.

Table 1. Selected Bond Distances and Angles for Complexes 3a, 3b, 4a, 5, and 7

	3a	3b	4a	5	7
			Bond Distances (Å)		
M−N(1)	2.02(1)	2.026(10)	2.049(3)	2.028(5)	2.020(6)
M−N(2)	2.03(1)	2.01(1)	2.038(3)	2.045(5)	2.004(5)
M−C(1)	2.48(2)	2.46(1)	2.480(4)	2.480(7)	2.451(7)
M−C(2)	2.47(2)	2.45(2)	2.474(4)	2.474(7)	2.464(7)
M−Cl(1)	2.488(4)	2.465(4)	2.483(1)	2.467(2)	2.494(2)
M−Cl(2)	2.473(4)	2.454(3)	2.494(1)	2.456(2)	2.490(2)
N(1)−C(1)	1.37(2)	1.38(2)	1.367(5)	1.373(8)	1.383(8)
N(2)−C(2)	1.37(2)	1.38(1)	1.371(5)	1.367(8)	1.383(8)
C(1)−C(2)	1.30(2)	1.36(2)	1.379(5)	1.389(10)	1.392(9)
M−CCP[a]	2.104	2.082	2.121	2.111	2.117
			Bond Angles (deg)		
N(1)−M−N(2)	81.4(5)	83.4(5)	82.8(1)	83.2(2)	84.0(2)
Cl(1)−M−Cl(2)	79.0(2)	79.9(1)	79.39(4)	78.64(8)	78.32(7)
N(1)−M−Cl(1)	86.1(4)	85.0(3)	83.76(9)	84.7(2)	84.3(2)
N(2)−M−Cl(2)	84.9(4)	83.3(3)	85.25(9)	84.4(2)	85.2(2)
M−N(1)−C(1)	91(1)	90.4(8)	90.9(2)	91.6(4)	90.1(4)
M−N(2)−C(2)	91.1(10)	90.6(8)	90.9(2)	90.7(4)	91.5(4)
N(1)−C(1)−C(2)	117(1)	117(1)	118.7(4)	117.6(6)	118.7(6)
N(2)−C(2)−C(1)	120(1)	120(1)	119.0(4)	119.8(6)	117.4(6)
dad−fold angle[b]	121.1(3)	120.0(3)	120.62(3)	121.1(3)	120.0(3)

[a] CCP = centroid of cyclopentadienyl ring. [b] dad−fold angle: dihedral angle between the N(1)−M−N(2) plane and N(1)−C(1)−C(2)−N(2) plane.

(18) Richter, B.; Scholz, J.; Sieler, J.; Thiele, K.-H. *Angew. Chem., Int. Ed. Engl.* **1995**, *34*, 2649.
(19) Durfee, L. D.; Hill, J. E.; Fanwick, P. E.; Rothwell, I. P. *Organometallics* **1990**, *9*, 75.
(20) Galakhov, M. V.; Gómez, M.; Jiménez, G.; Royo, P.; Pellinghelli, M. A.; Tiripicchio, A. *Organometallics* **1995**, *14*, 1901.
(21) Takai, K.; Ishiyama, T.; Yasue, H.; Nobunaka, T.; Itoh, M.; Oshiki, T.; Mashima, K.; Tani, K. *Organometallics* **1998**, *17*, 5128.
(22) Hubert-Pfalzgraf, L. G.; Zaki, A. *Acta Crystallogr.* **1993**, *C49*, 1609.

N^1-C^1 and N^2-C^2 distances are accordingly longer than those found for the *s-trans*-Cy-dad compound (1.258(2) Å).[10]

The $M-C^1$ and $M-C^2$ distances are short enough for the metal to make the π-interaction with the inner olefin carbons of the dad ligand; hence the fold angle θ between the planes defined by the atoms M, N^1, N^2 and N^1, C^1, C^2, N^2 lies in the range 120.0(3)−121.1(3)°; the values are unexceptionably comparable to those found for the related dad complexes of early transition metals.[24] The $M-N^1$ and $M-N^2$ distances are similar to those found for $NbCl_2Cp(\eta^4$-*supine*-^{t}Bu-dad) (2.015(4) and 2.021(4) Å)[22] and $TaCl_2Cp^*(\eta^4$-*supine*-^{i}Pr-dad) (2.000(4) and 2.006(4) Å).[14]

Alkylation of Dichloro Complexes of Niobium and Tantalum. The orientation of the dad ligand is mutable when the ligands on the tantalum, i.e., Cl or alkyl, were chosen. As shown in eq 1, the *supine*-dad ligand of **3a** and **6** flipped to the *prone* form in the dimethyl complexes $TaMe_2Cp^*(\eta^4$-*prone*-*p*-$MeOC_6H_4$-dad) (**10**) and $TaMe_2Cp^*(\eta^4$-*prone*-*o*-Tol-dad) (**11**), which were respectively derived from the reactions of **3a** and **6** with dimethylmagnesium in THF. It is not curious that reaction of the dichloro complexes **3a** or **6** with 2 equiv of MeMgI led to a complicated mixture including monomethyl derivatives since such partial alkylation has already been noted for some tantalum complexes.[3] The ^{1}H NMR spectrum of **10** and **11** displayed a singlet at δ 0.39 and 0.36, respectively, due to Ta−Me.[4] A singlet due to $H^{2,3}$ was observed at δ 5.84 for **10** and at δ 5.50 for **11**, being higher fields compared to that (δ 6.00) of the dichloro complexes **3a** and **6**. Thus, the chemical shift value of $H^{2,3}$ along with NOESY measurements indicated that **10** and **11** favored the *prone* orientation, which was further revealed by the X-ray analysis for **10** (vide infra).

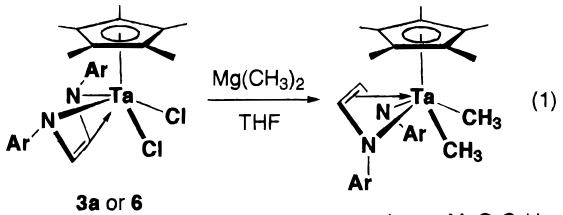

3a or **6**

10: Ar = *p*-MeO-C_6H_4
11: Ar = *o*-Tol

The reactions of the dad−dichloro complexes with $Mg(CH_2Ph)_2$ were then examined. The bis(benzyl) complexes of tantalum and niobium, $M(CH_2Ph)_2Cp^*(\eta^4$-*prone*-dad) (**12**, M = Ta, dad = *p*-$MeOC_6H_4$-dad; **13**, M = Nb, dad = *p*-$MeOC_6H_4$-dad; **14**, M = Ta, dad = Cy-dad), were obtained in modest yield from the reactions of the corresponding dichloro compounds, **3a**, **4a**, and **7**, with $Mg(CH_2Ph)_2$ in THF. The reaction of the *o*-Tol-dad complex **6** with an excess of $Mg(CH_2Ph)_2$ in diethyl ether did not give the corresponding bis(benzyl) complex $Ta(CH_2Ph)_2Cp^*(\eta^4$-*prone*-*o*-Tol-dad) (**15**); however, a mono(benzyl) complex $Ta(CH_2Ph)ClCp^*(\eta^4$-*supine*-*o*-Tol-dad) (**16**) was obtained in 43% yield instead, although we were able to prepare the dimethyl complex **11**. This might be ascribed to the congestion among the *o*-substituted dad ligand, the Cp* ligand, and the first introduced benzyl group. Structures of **12**−**14** and **16** were determined by NMR spectroscopy including NOESY measurements and further by the crystallographic studies for **14** and **16** (vide infra), indicating interesting structural features: the dad ligands of the complexes **12**−**14** preferred the *prone* orientation, the same geometry as that of the dimethyl complexes, while the complex **16** was found to be the *supine* one. Notably, such a delicate balance of the substituents on the tantalum atom can direct the orientation of the dad ligand. Thus, the dialkylation caused the change of the dad ligand from the *supine* conformation to the *prone* one.

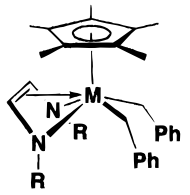

12: M = Ta R = *p*-MeO-C_6H_4
13: M = Nb R = *p*-MeO-C_6H_4
14: M = Ta R = Cy

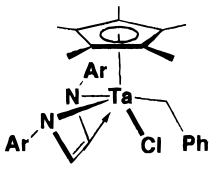

16: Ar = *o*-Tol

The bis(benzyl) complexes **12**−**14** thus isolated were thermally stable in the solid state, but in solution these complexes gradually decomposed to give the corresponding benzylidene complexes $M(=CHPh)Cp^*(\eta^4$-*prone*-dad) (**17**, M = Ta, dad = *p*-$MeOC_6H_4$-dad; **18**, M = Nb, dad = *p*-$MeOC_6H_4$-dad; **19**, M = Ta, dad = Cy-dad) with the release of toluene, monitored by the ^{1}H NMR spectra. These benzylidene complexes decomposed gradually during the attempted isolations, and hence these were characterized in solution by their NMR spectroscopy; the ^{1}H NMR spectra exhibited a characteristic α-benzylidene proton signal downfield of 7.95−8.49 ppm, suggesting the presence of a single rotamer. For the complex **19**, the most stable benzylidene complex among them, NOESY measurements clearly revealed that the methyl signal of the Cp* ligand was correlated with the $H^{2,3}$ protons of the dad ligand, the *ipso* protons of the two cyclohexyl groups, and the α-benzylidene proton, suggesting distinctly that the dad ligand kept the *prone* orientation and that the phenyl group of the benzylidene moiety pointed the direction opposite the Cp* ligand, an *anti*-rotamer. In the ^{13}C NMR spectrum, the benzylidene carbon atom of **19** appeared at δ 223 with a coupling constant J_{C-H} = 128.5 Hz.

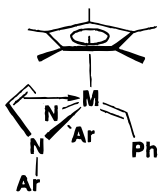

17: M = Ta
18: M = Nb
Ar = *p*-MeO-C_6H_4

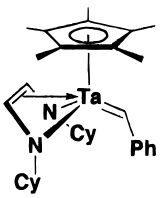

19

Crystal Structures of Alkylated Complexes 10, 14, and 16. The crystal structures of complexes **10**, **14**,

(23) Yasuda, H.; Tatsumi, K.; Okamoto, T.; Mashima, K.; Lee, K.; Nakamura, A.; Kai, Y.; Kanehisa, N.; Kasai, N. *J. Am. Chem. Soc.* **1985**, *107*, 2410.
(24) Scholz, J.; Dietrich, A.; Schumann, H.; Thiele, K.-H. *Chem. Ber.* **1991**, *124*, 1035.

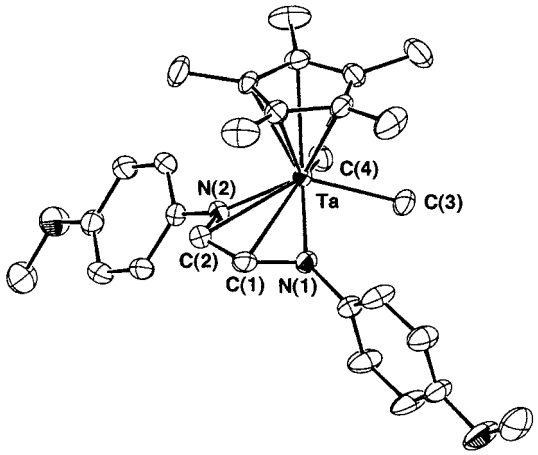

Figure 2. Molecular structure of **10** with the labeling scheme.

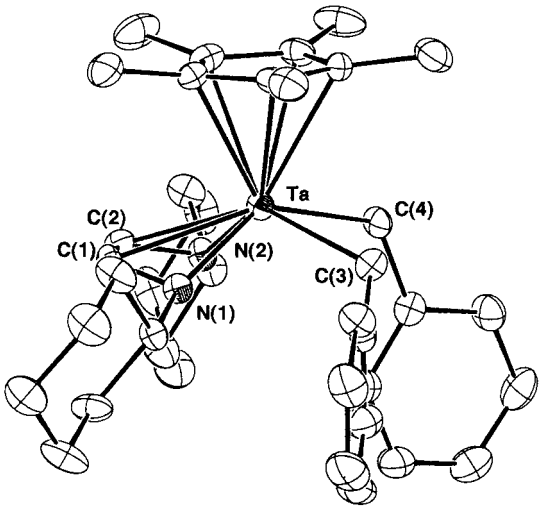

Figure 3. Molecular structure of **14** with the labeling scheme.

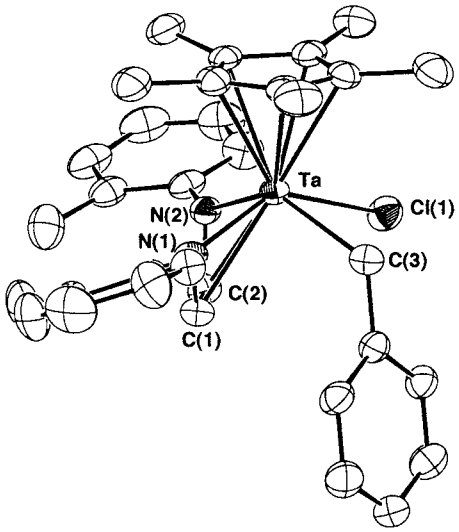

Figure 4. Molecular structure of **16** with the labeling scheme.

and **16** are given in Figures 2, 3, and 4, respectively, and selected metrical parameters are summarized in Table 2. Notable geometric features are that the complexes **10** and **14** adopt the *prone* conformation of the dad ligand as ascertained by the larger angles θ (127.3-(3)° for **10** and 122.8(3)° for **14**) between the planes defined by the atoms Ta, N^1, N^2 and N^1, C^1, C^2, N^2 and that in the monoalkylated complex **16** the *supine*-dad conformation is retained, as confirmed by the fold angle θ (118.8°), almost the same as that of the *supine*-dad complexes such as **3a**,**b**, **4a**, **5**, and **7**. The dissymmetry on the tantalum atom of **16** resulted in the different Ta−N distances. The Ta−N distance (2.047(6) Å) *trans* to a benzyl ligand is longer than that (2.008(6) Å) *trans* to a chloro ligand, being in good accordance with the tendency that Ta−N distances (av 2.04 Å) of dialkyl complexes **10** and **14** are slightly longer than those (av 2.02 Å) of the dichloro complexes **3a**,**b**, **4a**, **5**, and **7**.

Table 2. Selected Bond Distances and Angles for Complexes 10, 14, and 16

	10	**14**	**16**
	Bond Distances (Å)		
Ta−N(1)	2.024(4)	2.047(5)	2.008(6)
Ta−N(2)	2.064(4)	2.028(5)	2.047(6)
Ta−C(1)	2.555(6)	2.472(6)	2.439(7)
Ta−C(2)	2.548(6)	2.494(6)	2.477(7)
Ta−Cl(1)			2.495(2)
Ta−C(3)	2.242(6)	2.334(6)	2.324(7)
Ta−C(4)	2.213(6)	2.279(6)	
N(1)−C(1)	1.372(7)	1.376(7)	1.388(8)
N(2)−C(2))	1.379(7)	1.380(8)	1.371(8)
C(1)−C(2)	1.391(8)	1.361(9)	1.384(10)
Ta−CCP[a]	2.153	2.196	2.131
	Bond Angles (deg)		
N(1)−Ta−N(2)	83.2(2)	83.8(2)	82.9(2)
Cl(1)−Ta−C(3)			77.3(2)
C(3)−Ta−C(4)	75.5(2)	74.0(2)	
Ta−N(1)−C(1)	95.6(3)	90.3(4)	89.9(4)
Ta−N(2)−C(2)	93.4(3)	92.1(4)	90.7(5)
N(1)−C(1)−C(2)	117.0(5)	120.7(6)	119.3(7)
N(2)−C(2)−C(1)	120.5(5)	118.4(6)	116.9(7)
dad−fold angle[b]	127.3(3)	122.8(3)	118.6(3)

[a] CCP = centroid of cyclopentadienyl ring. [b] dad−fold angle: dihedral angle between the N(1)−Ta−N(2) plane and N(1)−C(1)−C(2)−N(2) plane.

In the *prone* complexes **10** and **14**, the Ta−C(dad) distances (2.555(6) and 2.548(6) Å for **10**; 2.472(6) and 2.494(6) Å for **14**) are longer than those (2.451(7)−2.480-(4) Å) found for the *supine* complexes **3a**,**b**, **4a**, **5**, and **7**, indicating that the π-donation of the C=C bond of the *prone*-dad is weaker than that of the *supine* one. The weaker π-interaction of the *prone*-butadiene ligand rather than the *supine* one has already been argued for the tantalum−bis(1,3-butadiene) complexes.[23] The Ta−C(alkyl) distances of the dimethyl complex **10** (2.242(6) and 2.213(6) Å) are slightly shorter than those (2.334-(6) and 2.279(6) Å) of the bis(benzyl) complex **14** and that (2.324(7) Å) of the monobenzyl complex **16**.

Synthesis and Characterization of 16-Electron dad−Butadiene Complexes. Introduction of a 1,3-butadiene ligand to the metal center led to the formation of 16-electron metalla-2,5-diazacyclopent-3-ene complexes. Treatment of **3a** with a slight excess of butadiene−magnesium adduct, which is a synthon of the diene dianion,[25,26] in THF developed the intense red color of

(25) (a) Fujita, K. Ohnuma, Y.; Yasuda, H.; Tani, H. *J. Organomet. Chem.* **1976**, *113*, 201. (b) Akutagawa, S.; Otsuka, S. *J. Am. Chem. Soc.* **1976**, *98*, 7420. (c) Yasuda, H.; Nakano, Y.; Natsukawa, K.; Tani, H. *Macromolecules* **1978**, *11*, 586. (d) Kai, Y.; Kanehisa, N.; Miki, K.; Kasai, N.; Mashima, K.; Yasuda, H.; Nakamura, A. *Chem. Lett.* **1982**, 1277.

the solution, from which a dark red mixed-ligand complex TaCp*(η^2-*N*,*N*′-*p*-$MeOC_6H_4$-dad)(η^4-*s*-*cis*-1,3-butadiene) (**20a**) was isolated in 52% yield. Similar treatments of **3b**, **4a**,**b**, and **5** afforded mixed-ligand complexes **20b**, **21a**,**b**, and **22**, respectively. A Cy-dad derivative **23** was also obtained in the same manner as a deep purple crystalline solid.

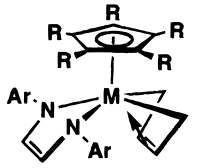

Ar = *p*-MeO-C_6H_4

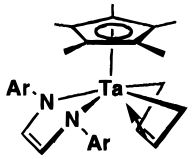

Ar = *p*-Tol

22

20a: M = Ta, R = Me
20b: M = Ta, R = H
21a: M = Nb, R = Me
21b: M = Nb, R = H

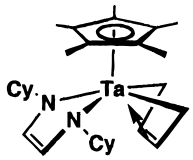

23

Spectroscopic data of these complexes are straightforward; their ^{1}H NMR spectra exhibited one set of signals due to both butadiene and dad ligands in exact 1:1 integral ratio. The dad ligand was found to be metalla-2,5-diazacyclopent-3-ene (mode A in Chart 1); the inner $H^{2,3}$ protons of the dad ligand were observed at much lower field (δ 6.71 for **20a**, δ 6.75 for **20b**, δ 6.67 for **21a**, δ 6.73 for **21b**, δ 6.73 for **22**, δ 6.68 for **23**) than those found for the dichloro complexes **3**−**7**, chemical shift values indicating the absence of the interaction between the olefinic C=C bond of the dad and the metal center. The butadiene ligand adopted a *supine*, η^4-*s*-*cis* conformation as judged by NMR spectroscopy; the chemical shift values of three kinds of butadiene protons were typical of the η^4-*s*-*cis*-diene coordination, and, in addition, the *supine* conformation of the butadiene ligand was indicated by the downfield-shifted central protons of the butadiene ligand. The *supine* conformation of the diene and the metallacyclic conformation of the dad were further revealed by X-ray analysis for the complexes **20a** and **23** (vide infra).

All complexes **20**−**23** showed characteristic intense red or purple color due to LMCT bands (512−542 nm), where the filled N(pπ) orbital is donated to the empty Ta(dπ*) orbital, in accordance with the metalla-2,5-diazacyclopent-3-ene structure (mode A). The pπ−dπ interaction somewhat stabilized the coordinative unsaturation around the 16-electron tantalum center of the complexes **20**−**23**. Such an intense color corresponds to the LMCT band of coordinatively unsaturated transition metal complexes, i.e., Cr,[27] Mo,[28,29] Re,[30] Ru,[31−42] Os,[43,44] Ir,[45,46] and Pd,[47] in which a filled pπ orbital of a heteroatom donates some electron densities to a vacant dπ orbital of metal as theoretically pointed out for 16-electron half-sandwich transition metal complexes.[48,49]

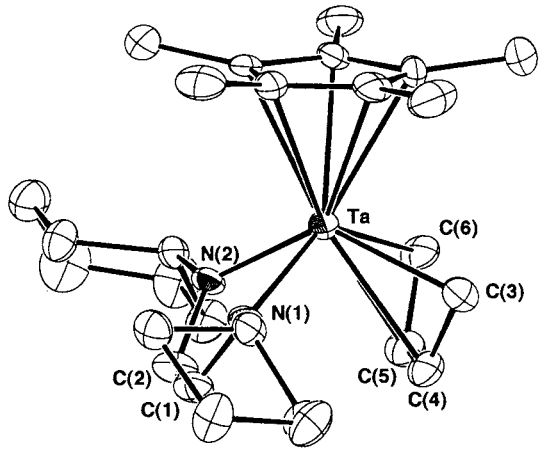

Figure 5. Molecular structure of **23** with the labeling scheme.

Crystal Structure of 16-Electron Mixed-Ligand Complexes 20a and 23. Single-crystal X-ray structural studies of **20a** and **23** revealed the constitution and geometry; the molecular view of **23** is shown in Figure 5, while that of **20a** has already been reported.[12] Selected metrical parameters of **20a** and **23** are given in Table 3. Half-metallocene complexes **20a** and **23** have

(26) (a) Rieke, R. D. *Science* **1989**, *246*, 1260. (b) Xiong, H.; Rieke, R. D. *J. Org. Chem.* **1989**, *54*, 3247. (c) Rieke, R. D.; Xiong, H. *J. Org. Chem.* **1991**, *56*, 3109. (d) Xiong, H.; Rieke, R. D. *Tetrahedron Lett.* **1991**, *32*, 5269. (e) Xiong, H.; Rieke, R. D. *J. Am. Chem. Soc.* **1992**, *114*, 4415. (f) Sell, M. S.; Xiong, H.; Rieke, R. D. *Tetrahedron Lett.* **1993**, *34*, 6011. (g) Sell, M. S.; Xiong, H.; Rieke, R. D. *Tetrahedron Lett.* **1993**, *34*, 6006.

(27) Sellmann, D.; Ludwig, W.; Huttner, G.; Zsolnai, L. *J. Organomet. Chem.* **1985**, *294*, 199.
(28) Ashby, M. T.; Enemark, J. H. *J. Am. Chem. Soc.* **1986**, *108*, 730.
(29) Cleland, W. E. J.; Barnhart, K. M.; Yamanouchi, K.; Collison, D.; Mabbs, F. E.; Ortega, R. B.; Enemark, J. H. *Inorg. Chem.* **1987**, *26*, 1017.
(30) Chang, L.; Aizawa, S.; Heeg, M. J.; Deutsch, E. *Inorg. Chem.* **1991**, *30*, 4920.
(31) Mashima, K.; Mikami, A.; Nakamura, A. *Chem. Lett.* **1992**, 1473.
(32) Mashima, K.; Kaneyoshi, H.; Kaneko, S.; Mikami, A.; Tani, K.; Nakamura, A. *Organometallics* **1997**, *16*, 1016.
(33) Mashima, K.; Kaneko, S.; Tani, K.; Kaneyoshi, H.; Nakamura, A. *J. Organomet. Chem.*, in press.
(34) Campion, B. K.; Heyn, R. H.; Tilley, T. D. *J. Chem. Soc., Chem. Commun.* **1988**, 278.
(35) Johnson, T. J.; Folting, K.; Streib, W. E.; Martin, J. D.; Huffman, J. C.; Jackson, S. A.; Eisenstein, O.; Caulton, K. G. *Inorg. Chem.* **1995**, *34*, 488.
(36) Catala, R.-M.; Cruz-Garritz, D.; Sosa, P.; Terreros, P.; Torrens, H.; Hills, A.; Hughes, D. L.; Richards, R. L. *J. Organomet. Chem.* **1989**, *359*, 219.
(37) Kölle, U.; Kossakowski, J. *J. Chem. Soc., Chem. Commun.* **1988**, 549.
(38) Koelle, U.; Kossakowski, J. *J. Organomet. Chem.* **1989**, *362*, 383.
(39) Koelle, U.; Rietmann, C.; Englert, U. *J. Organomet. Chem.* **1992**, *423*, C20.
(40) Loren, S. D.; Campion, B. K.; Heyn, R. H.; Tilley, T. D.; Bursten, B. E.; Luth, K. W. *J. Am. Chem. Soc.* **1989**, *111*, 4712.
(41) Takahashi, A.; Mizobe, Y.; Matsuzaka, H.; Dev, S.; Hidai, M. *J. Organomet. Chem.* **1993**, *456*, 243.
(42) Kee, T. P.; Park, L. Y.; Robbins, J.; Schrock, R. R. *J. Chem. Soc., Chem. Commun.* **1991**, 121.
(43) Michelman, R. I.; Andersen, R. A.; Bergman, R. G. *J. Am. Chem. Soc.* **1991**, *113*, 5100.
(44) Michelman, R. I.; Ball, G. E.; Bergman, R. G.; Andersen, R. A. *Organometallics* **1994**, *13*, 869.
(45) Garcia, J. J.; Torrens, H.; Adams, H.; Bailey, N. A.; Maitlis, P. M. *J. Chem. Soc., Chem. Commun.* **1991**, 74.
(46) Garcia, J. J.; Torrens, H.; Adams, H.; Bailey, N. A.; Scacklady, A.; Maitlis, P. M. *J. Chem. Soc., Dalton Trans.* **1993**, 1529.
(47) Mashima, K.; Kaneko, S.; Tani, K. *Chem. Lett.* **1997**, 347.
(48) Hofmann, P. *Angew. Chem., Int. Ed. Engl.* **1977**, *8*, 536.
(49) Siedle, A. R.; Newmark, R. A.; Pignolet, L. H.; Wang, D. X.; Albright, T. A. *Organometallics* **1986**, *5*, 38.

Table 3. Selected Bond Distances and Angles for Complexes 20a and 23

	20a	23
Bond Distances (Å)		
Ta−N(1)	2.128(4)	2.118(8)
Ta−N(2)	2.128(4)	2.116(9)
Ta−C(3)	2.267(6)	2.26(1)
Ta−C(4)	2.402(7)	2.42(1)
Ta−C(5)	2.411(6)	2.41(1)
Ta−C(6)	2.280(6)	2.26(1)
N(1)−C(1)	1.387(7)	1.35(1)
N(2)−C(2)	1.381(7)	1.36(1)
C(1)−C(2)	1.323(8)	1.35(2)
C(3)−C(4)	1.43(1)	1.42(2)
C(5)−C(6)	1.44(1)	1.43(2)
C(4)−C(5)	1.36(1)	1.39(2)
Ta−CCP[c]	2.120	2.139
Bond Angles (deg)		
N(1)−Ta−N(2)	75.6(2)	75.1(3)
C(3)−Ta−C(6)	74.3(3)	76.7(5)
Ta−N(1)−C(1)	110.4(4)	112.0(7)
Ta−N(2)−C(2)	110.4(4)	114.4(7)
N(1)−C(1)−C(2)	117.6(5)	117.0(10)
N(2)−C(2)−C(1)	117.8(5)	116(1)
dad−fold angle[a]	154.9(3)	155.9(3)
bd−fold angle[b]	95.8(3)	98.9(3)

[a] dad−fold angle: dihedral angle between the N(1)−Ta−N(2) plane and N(1)−C(1)−C(2)−N(2) plane. [b] bd−fold angle: dihedral angle between the C(3)−Ta−C(6) plane and C(3)−C(4)−C(5)−C(6) plane. [c] CCP = centroid of cyclopentadienyl ring.

one *supine*-η^4-*s*-*cis*-1,3-butadiene ligand and one η^2-*N*,*N*′-endiamido^{2-} ligand (mode A); thus the dad coordination mode is distinctly different from the *supine*- and *prone*-σ^2,π-endiamido structure (mode B) of the dad ligand found for dichloro and dialkyl complexes (vide supra). The trigonal planar nitrogen atom is preferred to make the pπ−dπ interaction with the metal center; the sums of three angles around the nitrogen atoms are N^1 = 359.8° and N^2 = 360.0° for **20a** and N^1 = 359.6° and N^2 = 358.8° for **23**. The fold angle θ (154.9(3)° for **20a** and 155.9(3)° for **23**) between the planes defined by the atoms Ta, N^1, N^2 and N^1, C^1, C^2, N^2 is larger than that (140.8°) of $ZrCp_2(\eta^2$-*N*,*N*′-Ph_4-dad) (Ph_4-dad = 1,2,3,4-tetraphenyl-1,4-diaza-1,3-butadiene),[50] an isoelectronic analogy to **20**−**23**, indicating that the five-membered ring system is not so puckered, but is deformed away from the Cp* ligand so as to minimize the steric congestion.

The Ta−N distances (2.128(4) and 2.128(4) Å for **20a**, 2.118(8) and 2.116(9) Å for **23**) are substantially longer than those of dichloro complexes **3a**,**b**, **4a**, **5**, and **7** (av 2.02 Å), dialkyl complexes **10** and **14** (av 2.04 Å), and a monoalkyl complex **16** (av 2.03 Å). The N−Ta−N bite angle of the dad ligand is 75.6(2)° for **20a** and 75.1(3)° for **23**, being smaller than that of the dichloro complexes (av 83.0°), the dialkyl complexes (av 83.5°), and the monoalkyl complex (82.9(2)°). These findings may be attributed to a partial contribution of mode C (Chart 1), although a group 6 metal complex $WCl_2(N^tBu)(^tBu$-dad), which is a typical example of a dad complex having the mode C structure, has much longer W−N distances (2.507(7) and 2.533(7) Å), and a much narrower N−W−N bite angle (67.0(2)°).[51]

The butadiene ligand bound to the tantalum atom usually has *supine*-s-cis-η^4-coordination.[23] The short−long−short C−C bond sequence of the butadiene moiety is also normal for the diene complexes of early transition metals having a large contribution of metallacyclopentene canonical form, being in good accordance with the obstacle hold angle (95.8(3)° for **20a**, 98.9(3)° for **23**) between the planes defined by the atoms Ta, C^3, C^6 and C^3, C,[4] C,[5] C.[6]

Conclusion

In this contribution, we have synthesized and characterized various half-sandwich complexes of niobium and tantalum bearing a 1,4-diaza-1,3-butadiene ligand and have established that the coordination mode of the dad ligand in the half-metallocene complexes is mutually alterable; three modes A, B, and D (Chart 1), and additionally, for the mode B, two conformations, *supine* and *prone*, are demonstrated. The coordination mode of the dad ligand depends sensitively on the ligand environment at the metal center. Dichloro complexes, **3**−**7**, adopt a *supine*-σ^2,π-endiamido structure (*supine*-B), while a dichloro $(^iPr)_2C_6H_3$-dad complex **9** favors the η^2-*C*,*N*-coordination (mode D) due to the bulky *N*-substituted ligand. Reactions of dichloro complexes with $MgMe_2$ and $Mg(CH_2Ph)_2$ gave dimethyl complexes **10** and **11** and dibenzyl complexes **12**−**14**. During the reaction course, the *supine* orientation of the dad ligand bound to the metal was flipped to the *prone* one (*prone*-B). Noteworthy is that this turn of the dad ligand requires dialkylation, in sharp contrast to the steric control of preferential conformation of the dad ligand,[14] since monobenzylation resulted in the formation of the *supine* complex **16**. In 16-electron complexes **20**−**23**, the introduction of a diene ligand resulted in the formation of the metallacyclic structure of the dad ligand (mode A), in which the metal center has no direct π-interaction with the inner two carbons of the dad ligand. The coordinative unsaturation around the metal center having the mode A dad ligand was stabilized by the donation of the filled pπ(N) orbital to the vacant dπ-(metal) orbital; their LMCT band appeared around 512−542 nm. Thus, the adequate flexibility (hapticity and conformation) of the dad ligand may be expected to play a unique role in the catalytic process.

Experimental Section

General Procedures. All manipulations involving air- and moisture-sensitive organometallic compounds were carried using standard Schlenk techniques under argon. Complexes $MCl_4(\eta^5$-$C_5R_5)$ (M = Ta, R = CH_3 (**1a**); M = Ta, R = H (**1b**); M = Nb, R = CH_3 (**2a**); M = Nb, R = H (**2b**)) were prepared according to the literature.[52] Hexane, THF, and toluene were dried and deoxygenated by distillation over sodium benzophenone ketyl under argon. Benzene-d_6 and THF-d_8 were distilled from Na/K alloy and thoroughly degassed by trap-to-trap distillation before use. 1,4-Diaza-1,3-butadiene ligands (*N*,*N*′-disubstituted aliphatic and aromatic diimines) were prepared according to the literature.[53] A low-valent tantalum complex, $[TaCl_2Cp^*]_2$ (**8**), was prepared according to the literature.[16,17]

(50) Scholz, J.; Dlikan, M.; Ströhl, D.; Dietrich, A.; Schumann, H.; Thiele, K.-H. *Chem. Ber.* **1990**, *123*, 2279.

(51) Dreisch, K.; Andersson, C.; Stålhandske, C. *Polyhedron* **1993**, *12*, 1335.

(52) Cardoso, A. M.; Clark, R. J. H.; Moorhouse, S. *J. Chem. Soc., Dalton Trans.* **1980**, 1156.

(53) Kliegman, J. M.; Barnes, R. K. *Tetrahedron* **1970**, *26*, 2555. Kliegman, J. M.; Barnes, R. K. *J. Org. Chem.* **1970**, *35*, 3140. Van Koten, G.; Vrieze, K. *Adv. Organomet. Chem.* **1982**, *21*, 151.

The ^{1}H (500, 400, 300, and 270 MHz) and ^{13}C (125, 100, 75, and 68 MHz) NMR spectra in C_6D_6 were measured on a Varian Unity Inova-500, a JEOL JNM-AL400, a Varian Mercury-300, or a JEOL GSX-270 spectrometer. When benzene-d_6 was used as the solvent, the spectra were referenced to the residual solvent protons at δ 7.20 in the ^{1}H NMR spectra and to the residual solvent carbons at δ 128.0 in the ^{13}C NMR spectra. When THF-d_8 was used as the solvent, the spectra were referenced to the residual solvent protons at δ 1.73 in the ^{1}H NMR spectra and to the residual solvent carbons at δ 25.2 in the ^{13}C NMR spectra. Assignments for ^{1}H and ^{13}C NMR peaks for some of the complexes were aided by 2D ^{1}H−^{1}H COSY, 2D ^{1}H−^{1}H NOESY, and 2D ^{1}H−^{13}C HMQC spectra, respectively. Other spectra were recorded by the use of the following instruments: IR, JASCO FT/IR-230; low- and high-resolution mass spectra, JEOL SX-102; UV/vis spectra, JASCO V-570; elemental analyses, Perkin-Elmer 2400. All melting points were measured in sealed tubes under argon atmosphere and were not corrected.

Preparation of $TaCl_2Cp^*$(*p*-MeOC$_6$H$_4$-dad) (3a). A solution of Li_2(MeOC$_6$H$_4$-dad)(thf)$_4$ (2.35 mmol) in THF (20 mL) was added to a solution of **1a** (1.03 g, 2.24 mmol) in THF (20 mL) at −78 °C. The reaction mixture was allowed to warm to room temperature and then was stirred for 6 h at 25 °C. All volatiles were removed under reduced pressure to leave a residue, which was washed with eight portions of THF (2 mL), giving **3a** as yellow microcrystals in 40% yield, mp 237−246 °C (dec). ^{1}H NMR (270 MHz, C_6D_6, 35 °C): δ 2.08 (s, 15H, C_5Me_5), 3.41 (s, 6H, OCH_3), 6.00 (s, 2H, N=CH−), 6.86 (m, 4H, *m*-C_6H_4), 7.42 (m, 4H, *o*-C_6H_4). ^{13}C NMR (100 MHz, C_6D_6, 35 °C): δ 12.6 (q, $^1J_{C-H}$ = 128 Hz, C_5Me_5), 55.1 (q, $^1J_{C-H}$ = 143 Hz, OCH_3), 110.8 (d, $^1J_{C-H}$ = 182 Hz, N=CH−), 113.7 (d, $^1J_{C-H}$ = 159 Hz, *m*-C_6H_4), 121.9 (s, C_5Me_5), 127.1 (d, $^1J_{C-H}$ = 161 Hz, *o*-C_6H_4), 143.9 (s, *ipso*-C_6H_4), 158.3 (s, *p*-C_6H_4). IR (KBr): ν(CN)/cm^{-1} 1505 (s). Anal. Calcd for $C_{26}H_{31}Cl_2N_2O_2Ta$: C, 47.65; H, 4.77; N, 4.27. Found: C, 47.51; H, 4.79; N, 4.60.

Similar procedures were used for the synthesis of **3b**, **4a**, and **4b**.

3b: 46% yield, mp 190−220 °C (dec). ^{1}H NMR (270 MHz, C_6D_6, 35 °C): δ 3.42 (s, 6H, OCH_3), 6.08 (s, 5H, C_5H_5), 6.09 (s, 2H, N=CH−), 6.88 (m, 4H, *m*-C_6H_4), 7.22 (m, 4H, *o*-C_6H_4). ^{13}C NMR (100 MHz, THF-d_8, 35 °C): δ 55.6 (q, $^1J_{C-H}$ = 143 Hz, OCH_3), 110.8 (d, $^1J_{C-H}$ = 182 Hz, N=CH−), 111.6 (d, $^1J_{C-H}$ = 181 Hz, C_5H_5), 114.6 (d, $^1J_{C-H}$ = 159 Hz, *m*-C_6H_4), 125.4 (d, $^1J_{C-H}$ = 160 Hz, *o*-C_6H_4), 144.4 (s, *ipso*-C_6H_4), 158.8 (s, *p*-C_6H_4). IR (KBr): ν(CN)/cm^{-1} 1511 (s). Anal. Calcd for $C_{21}H_{21}Cl_2N_2O_2Ta$: C, 43.10; H, 3.62; N, 4.79. Found: C, 42.79; H, 3.84; N, 4.87.

4a: 32% yield, mp 187−191 °C (dec). ^{1}H NMR (400 MHz, C_6D_6, 35 °C): δ 1.95 (s, 15H, C_5Me_5), 3.40 (s, 6H, OCH_3), 6.05 (s, 2H, N=CH−), 6.84 (m, 4H, *m*-C_6H_4), 7.47 (m, 4H, *o*-C_6H_4). ^{13}C NMR (100 MHz, C_6D_6, 35 °C): δ 13.3 (q, $^1J_{C-H}$ = 129 Hz, C_5Me_5), 55.2 (q, $^1J_{C-H}$ = 144 Hz, OCH_3), 112.8 (d, $^1J_{C-H}$ = 181 Hz, N=CH−), 113.7 (d, $^1J_{C-H}$ = 159 Hz, *m*-C_6H_4), 124.1 (s, C_5Me_5), 126.5 (d, $^1J_{C-H}$ = 161 Hz, *o*-C_6H_4), 144.5 (s, *ipso*-C_6H_4), 158.5 (s, *p*-C_6H_4). IR (KBr): ν(CN)/cm^{-1} 1504 (s). Anal. Calcd for $C_{26}H_{31}Cl_2N_2O_2Nb$: C, 55.04; H, 5.51; N, 4.94. Found: C, 55.01; H, 5.63; N, 5.05.

4b: 18% yield, mp 172−183 °C (dec). ^{1}H NMR (400 MHz, C_6D_6, 35 °C): δ 3.40 (s, 6H, OCH_3), 6.12 (s, 5H, C_5H_5), 6.19 (s, 2H, N=CH−), 6.85 (m, 4H, *m*-C_6H_4), 7.27 (m, 4H, *o*-C_6H_4). ^{13}C NMR (100 MHz, C_6D_6, 35 °C): δ 55.3 (OCH_3), 111.9 (C_5H_5), 112.2 (N=CH−), 114.6 (*m*-C_6H_4), 124.8 (*o*-C_6H_4), 144.9 (*ipso*-C_6H_4), 158.8 (*p*-C_6H_4). IR (KBr): ν(CN)/cm^{-1} 1504 (s). Anal. Calcd for $C_{21}H_{21}Cl_2N_2O_2Nb$: C, 50.73; H, 4.26; N, 5.63. Found: C, 50.51; H, 4.61; N, 5.93.

Preparation of $TaCl_2Cp^*$(*p*-Tol-dad) (5). A solution of Li_2(*p*-Tol-dad)(thf)$_4$ (2.72 mmol) in THF (15 mL) was added to a solution of **1a** (1.19 g, 2.59 mmol) in THF (10 mL) at −78 °C. The reaction mixture was allowed to warm to room temperature with magnetic stirring. After the mixture was stirred for 16 h at 25 °C, all volatiles were removed under reduced pressure to give a residue, which was washed with five portions of THF (2 mL), giving **5** as yellow microcrystals, 57% yield, mp 258−261 °C (dec). ^{1}H NMR (400 MHz, C_6D_6, 35 °C): δ 2.07 (s, 15H, C_5Me_5), 2.23 (s, 6H, CH_3), 6.00 (s, 2H, N=CH−), 7.07 (m, 4H, *p*-C_6H_4), 7.39 (m, 4H, *o*-C_6H_4). ^{13}C NMR (100 MHz, C_6D_6, 35 °C): δ 12.8 (q, $^1J_{C-H}$ = 128 Hz, C_5Me_5), 21.0 (q, $^1J_{C-H}$ = 126 Hz, CH_3), 110.8 (d, $^1J_{C-H}$ = 182 Hz, N=CH−), 122.1 (s, C_5Me_5), 126.0 (d, $^1J_{C-H}$ = 165 Hz, *o*-C_6H_4), 129.6 (d, $^1J_{C-H}$ = 159 Hz, *m*-C_6H_4), 135.5 (s, *p*-C_6H_4), 148.3 (s, *ipso*-C_6H_4). IR (KBr): ν(CN)/cm^{-1} 1505 (s). Anal. Calcd for $C_{26}H_{31}Cl_2N_2Ta$: C, 50.09; H, 5.01; N, 4.49. Found: C, 49.77; H, 4.99; N, 4.55.

Preparation of $TaCl_2Cp^*$(*o*-Tol-dad) (6). To a solution of **1a** (1.86 g, 4.05 mmol) in THF (16 mL) cooled at −78 °C was added a solution of Li_2(*o*-Tol-dad)(thf)$_4$ (1.05 equiv, 4.26 mmol) in THF (16 mL). The reaction mixture was allowed to warm to room temperature and was stirred for 10 h at room temperature. All volatiles were removed under reduced pressure. Complex **6** was obtained as yellow microcrystals, 74% yield, mp 155−158 °C (dec). ^{1}H NMR (400 MHz, C_6D_6, 35 °C): δ 1.84 (s, 6H, CH_3), 1.97 (s, 15H, C_5Me_5), 5.79 (s, 2H, N=CH−), 7.05 (d, 2H, 3-C_6H_4), 7.06 (t, 2H, 4-C_6H_4), 7.23 (t, 2H, 5-C_6H_4), 8.62 (d, 2H, 6-C_6H_4). ^{13}C NMR (100 MHz, C_6D_6, 35 °C): δ 12.0 (q, $^1J_{C-H}$ = 128 Hz, C_5Me_5), 19.1 (q, $^1J_{C-H}$ = 127 Hz, CH_3), 110.4 (d, $^1J_{C-H}$ = 183 Hz, N=CH−), 122.2 (s, C_5Me_5), 126.0 (d, $^1J_{C-H}$ = 163 Hz, 6-C_6H_4), 126.4 (d, $^1J_{C-H}$ = 162 Hz, 5-C_6H_4), 126.6 (d, $^1J_{C-H}$ = 161 Hz, 3-C_6H_4), 130.2 (d, $^1J_{C-H}$ = 159 Hz, 4-C_6H_4), 134.7 (s, 2-C_6H_4), 149.3 (s, 1-C_6H_4). IR (KBr): ν(CN)/cm^{-1} 1486 (s). Anal. Calcd for $C_{26}H_{31}Cl_2N_2Ta$: C, 50.09; H, 5.01; N, 4.49. Found: C, 50.00; H, 5.16; N, 4.16.

Preparation of $TaCl_2Cp^*$(Cy-dad) (7). A solution of Li_2(Cy-dad)(thf)$_4$ (0.672 mmol) in THF (8.0 mL) was added to a solution of **1a** (293 mg, 0.640 mmol) in THF (8.0 mL) at −78 °C. The reaction mixture was allowed to warm to room temperature. After the mixture was stirred for 10 h at 25 °C, all volatiles were removed under reduced pressure to leave a residue, which was washed with five portions of THF (2 mL) to give **7** as yellow microcrystals, 60% yield, mp 160−163 °C (dec). ^{1}H NMR (400 MHz, C_6D_6, 35 °C): δ 1.05, 1.25, 1.49, 1.56, 1.64, 1.85, 2.95, and 3.99 (m, 22H, cyclohexyl protons), 2.16 (s, 15H, C_5Me_5), 6.22 (s, 2H, N=CH−). ^{13}C NMR (100 MHz, C_6D_6, 35 °C): δ 11.8 (q, $^1J_{C-H}$ = 128 Hz, C_5Me_5), 26.2, 26.5, 26.7, 27.6, 39.4, and 64.0 (cyclohexyl carbons), 105.1 (d, $^1J_{C-H}$ = 178 Hz, N=CH−), 120.5 (s, C_5Me_5). IR (KBr): ν(CN)/cm^{-1} 1453 (s). Anal. Calcd for $C_{24}H_{39}Cl_2N_2Ta$: C, 47.46; H, 6.47; N, 4.61. Found: C, 47.34; H, 6.43; N, 4.46.

Preparation of $TaCl_2Cp^*(\eta^2$-(^{i}Pr)$_2$C$_6$H$_3$-dad) (9). Complex **8** (6.5 mg, 0.0084 mmol) and (^{i}Pr)$_2$C$_6$H$_3$-dad (3.2 mg, 0.0084 mmol) were dissolved in 0.58 mL of C_6D_6 in a 5 mm NMR tube. After stirring at 35 °C for 12 h, the η^2-imine complex **9** was formed. ^{1}H NMR (400 MHz, C_6D_6, 35 °C): δ 1.09 (d, 3H, CH(CH_3)(CH$_3$)), 1.10 (d, 3H, CH(CH$_3$)(CH_3)), 1.14 (d, 6H, CH(CH_3)$_2$), 1.24 (d, 6H, CH(CH_3)$_2$), 1.41 (d, 3H, CH(CH_3)(CH$_3$)), 1.55 (d, 3H, CH(CH$_3$)(CH_3)), 2.07 (s, 15H, C_5Me_5), 2.34 (m, 1H, CH(CH$_3$)$_2$), 3.16 (m, 2H, CH(CH$_3$)$_2$), 3.67 (d, $^3J_{H-H}$ = 7.3 Hz, 1H, N=CH− (coordinated)), 4.29 (m, 1H, CH(CH$_3$)$_2$), 7.15 (m, 6H, C_6H_3), 7.73 (d, $^3J_{H-H}$ = 7.3 Hz, 1H, N=CH− (free)).

Preparation of $TaMe_2Cp^*$(*p*-MeOC$_6$H$_4$-dad) (10) and $TaMe_2Cp^*$(*o*-Tol-dad) (11). A solution of $MgMe_2$ (2.01 mmol) in THF (1.8 mL) was added to a solution of **3a** (881 mg, 1.34 mmol) in THF (50 mL) at −78 °C. The reaction mixture was allowed to warm to room temperature. After the mixture was stirred for 6 h at 25 °C, all volatiles were removed under reduced pressure to give a residue, from which the product was extracted into 20 portions of hexane (60 mL). Concentration of the solution to ca. 5 mL gave **10** as yellow microcrystals in 81% yield, mp 116−123 °C (dec). ^{1}H NMR (400 MHz, C_6D_6, 35 °C): δ 0.39 (s, 6H, Ta−CH_3), 1.84 (s, 15H, C_5Me_5), 3.42 (s, 6H, OCH_3), 5.84 (s, 2H, N=CH−), 6.90 (m, 4H, *m*-C_6H_4), 7.12

(m, 4H, *o*-C_6H_4). ^{13}C NMR (100 MHz, C_6D_6, 35 °C): δ 11.3 (q, $^1J_{C-H}$ = 127 Hz, C_5Me_5), 44.2 (q, $^1J_{C-H}$ = 118 Hz, Ta−CH_3), 55.0 (q, $^1J_{C-H}$ = 143 Hz, OCH_3), 107.1 (d, $^1J_{C-H}$ = 174 Hz, N=CH−), 114.1 (d, $^1J_{C-H}$ = 157 Hz, *m*-C_6H_4), 114.9 (s, C_5Me_5), 124.8 (d, $^1J_{C-H}$ = 157 Hz, *o*-C6H4), 145.6 (s, *ipso*-C_6H_4), 156.6 (s, *p*-C_6H_4). IR (KBr): ν(CN)/cm^{-1} 1502 (s). Anal. Calcd for $C_{28}H_{37}N_2O_2Ta$: C, 54.72; H, 6.07; N, 4.56. Found: C, 54.66; H, 6.26; N, 4.45.

A similar reaction afforded **11** as yellow microcrystals.

11: 76% yield, mp 147−149 °C (dec). ^{1}H NMR (400 MHz, C_6D_6, 35 °C): δ 0.36 (s, 6H, Ta−CH_3), 1.78 (s, 15H, C_5Me_5), 2.23 (s, 6H, CH_3), 5.50 (s, 2H, N=CH−), 7.04 (t, 2H, 4-C_6H_4), 7.08 (d, 2H, 6-C_6H_4), 7.19 (d, 2H, 3-C_6H_4), 7.22 (t, 2H, 5-C_6H_4). ^{13}C NMR (100 MHz, C_6D_6, 35 °C): δ 11.1 (q, $^1J_{C-H}$ = 127 Hz, C_5Me_5), 19.0 (q, $^1J_{C-H}$ = 127 Hz, CH_3), 44.8 (q, $^1J_{C-H}$ = 120 Hz, Ta−CH_3), 105.2 (d, $^1J_{C-H}$ = 175 Hz, N=CH−), 114.1 (s, C_5Me_5), 124.4 (d, $^1J_{C-H}$ = 156 Hz, 6-C_6H_4), 124.9 (d, $^1J_{C-H}$ = 161 Hz, 4-C_6H_4), 126.0 (d, $^1J_{C-H}$ = 159 Hz, 5-C_6H_4), 131.1 (d, $^1J_{C-H}$ = 157 Hz, 3-C_6H_4), 135.8 (s, 2-C_6H_4), 151.3 (s, 1-C_6H_4). IR (KBr): ν(CN)/cm^{-1} 1485 (s). Anal. Calcd for $C_{28}H_{37}N_2Ta$: C, 57.73; H, 6.40; N, 4.81. Found: C, 57.86; H, 6.07; N, 4.83.

Preparation of M(CH_2Ph)$_2$Cp*(*p*-MeOC_6H_4-dad) (12, M = Ta; 13, M = Nb) and Ta(CH_2Ph)$_2$Cp*(Cy-dad) (14). To a solution of **3a** (1.00 g, 1.53 mmol) in THF (30 mL) cooled at −78 °C was added a solution of Mg(CH_2Ph)$_2$ (1.83 mmol) in THF (10 mL) via syringe. After the mixture was stirred for 3 h at 25 °C, all volatiles were removed under reduced pressure. The resulting residue was extracted with 10 portions of hexane (60 mL). Concentration of the solution gave **12** as yellow microcrystals in 91% yield, mp 57−63 °C (dec). ^{1}H NMR (400 MHz, C_6D_6, 35 °C): δ 1.88 (s, 15H, C_5Me_5), 1.99 (d, $^2J_{H-H}$ = 10.7 Hz, 2H, CH_2Ph), 2.16 (d, $^2J_{H-H}$ = 10.7 Hz, 2H, CH_2Ph), 3.41 (s, 6H, OCH_3), 5.78 (s, 2H, N=CH−), 6.82 (t, $^3J_{H-H}$ = 7.6 Hz, 2H, *p*-C_6H_5), 6.85 (s, 8H, *o*- and *m*-C_6H_4), 6.90 (d, $^3J_{H-H}$ = 7.6 Hz, 4H, *o*-C_6H_5), 7.07 (t, $^3J_{H-H}$ = 7.6 Hz, 4H, *m*-C_6H_5). ^{13}C NMR (100 MHz, C_6D_6, 35 °C): δ 12.2 (q, $^1J_{C-H}$ = 127 Hz, C_5Me_5), 55.1 (q, $^1J_{C-H}$ = 143 Hz, OCH_3), 61.9 (t, $^1J_{C-H}$ = 122 Hz, CH_2Ph), 110.5 (d, $^1J_{C-H}$ = 178 Hz, N=CH−), 113.7 (d, $^1J_{C-H}$ = 158 Hz, *m*-C_6H_4), 118.1 (s, C_5Me_5), 122.0 (d, $^1J_{C-H}$ = 156 Hz, *p*-C_6H_5), 124.8 (d, $^1J_{C-H}$ = 158 Hz, *o*-C_6H_4), 126.9 (d, $^1J_{C-H}$ = 157 Hz, *m*-C_6H_5), 128.9 (d, $^1J_{C-H}$ = 156 Hz, *o*-C_6H_5), 144.5 (s, *ipso*-C_6H_4), 153.9 (s, *ipso*-C_6H_5), 156.7 (s, *p*-C_6H_4). IR (KBr): ν(CN)/cm^{-1} 1503 (s). Anal. Calcd for $C_{40}H_{45}N_2O_2Ta$: C, 62.66; H, 5.92; N, 3.65. Found: C, 62.40; H, 6.31; N, 3.34.

Similar procedures were used for the synthesis of **13** and **14**.

13: red crystals in 96% yield, mp 49−52 °C (dec). ^{1}H NMR (400 MHz, C_6D_6, 35 °C): δ 1.81 (s, 15H, C_5Me_5), 2.12 (d, $^2J_{H-H}$ = 10.7 Hz, 2H, CH_2Ph), 2.34 (d, $^2J_{H-H}$ = 10.7 Hz, 2H, CH_2-Ph), 3.41 (s, 6H, OCH_3), 5.79 (s, 2H, N=CH−), 6.6−7.2 (18H, aromatic protons). Anal. Calcd for $C_{40}H_{45}N_2O_2Nb$: C, 70.79; H, 6.68; N, 4.13. Found: C, 70.50; H, 7.04; N, 4.36.

14: yellow crystals in 83% yield, mp 146−149 °C (dec). ^{1}H NMR (400 MHz, C_6D_6, 35 °C): δ 1.0−1.8 (m, 20H, Cy), 1.74 (s, 15H, C_5Me_5), 2.36 (d,$^2J_{H-H}$ = 12.9 Hz, 2H, CH_2Ph), 2.55 (d,$^2J_{H-H}$ = 12.9 Hz, 2H, CH_2Ph), 3.86 (m, 2H, Cy), 5.61 (s, 2H, N=CH−), 6.97 (t, $^3J_{H-H}$ = 7.3 Hz, 2H, *p*-C_6H_5), 7.21 (t, $^3J_{H-H}$ = 7.3 Hz, 4H, *m*-C_6H_5), 7.32 (d, $^3J_{H-H}$ = 7.3 Hz, 4H, *o*-C_6H_5). ^{13}C NMR (100 MHz, C_6D_6, 35 °C): δ 11.7 (q, $^1J_{C-H}$ = 127 Hz, C_5Me_5), 26.3 (t, $^1J_{C-H}$ = 127 Hz, Cy), 26.4 (t, $^1J_{C-H}$ = 128 Hz, Cy), 26.6 (t, $^1J_{C-H}$ = 128 Hz, Cy), 33.7 (t, $^1J_{C-H}$ = 126 Hz, Cy), 37.1 (t, $^1J_{C-H}$ = 126 Hz, Cy), 59.1 (d, $^1J_{C-H}$ = 136 Hz, Cy), 65.3 (t, $^1J_{C-H}$ = 118 Hz, CH_2Ph), 99.6 (d, $^1J_{C-H}$ = 166 Hz, N=CH−), 114.4 (s, C_5Me_5), 122.7 (d, $^1J_{C-H}$ = 156 Hz, *p*-C_6H_5), 127.2 (d, $^1J_{C-H}$ = 157 Hz, *m*-C_6H_5), 131.7 (d, $^1J_{C-H}$ = 155 Hz, *o*-C_6H_5), 151.7 (s, *ipso*-C_6H_5). IR (KBr): ν(CN)/cm^{-1} 1447 (s). Anal. Calcd for $C_{38}H_{53}N_2Ta$: C, 63.50; H, 7.43; N, 3.90. Found: C, 63.67; H, 7.48; N, 3.96.

Preparation of Ta(CH_2Ph)ClCp*(*o*-Tol-dad) (16). To a solution of **6** (172 mg, 0.276 mmol) in THF (30 mL) cooled at −78 °C was added a solution of Mg(CH_2Ph)$_2$ (2.2 equiv, 0.607 mmol) in diethyl ether (2.0 mL) via syringe. The reaction mixture was stirred for 8 h at 25 °C. Removal of all volatiles under reduced pressure afforded a residue, which was extracted into four portions of hexane (60 mL). Concentration of the solution gave yellow **16** as microcrystals (43% yield), mp 158−162 °C (dec). ^{1}H NMR (400 MHz, C_6D_6, 35 °C): δ 1.81 (s, 3H, CH_3), 1.86 (s, 3H, CH_3) 1.87 (s, 15H, C_5Me_5), 2.09 (d, $^2J_{H-H}$ = 9.5 Hz, 1H, CH_2Ph), 2.42 (d, $^2J_{H-H}$ = 9.5 Hz, 1H, CH_2Ph), 5.11 (d, $^3J_{H-H}$ = 2.9 Hz, 1H, N=CH−), 5.48 (d, $^3J_{H-H}$ = 2.9 Hz, 1H, N=CH−), 6.81 (t, $^3J_{H-H}$ = 7.8 Hz, 1H, *p*-C_6H_5), 7.03 (d, 1H, 3-C_6H_4 *trans* to Cl), 7.04 (d, 1H, 3-C_6H_4 *trans* to CH_2-Ph), 7.07 (t, 1H, 4-C_6H_4 *trans* to Cl), 7.08 (t, 1H, 4-C_6H_4 *trans* to CH_2Ph), 7.21 (t, 1H, 5-C_6H_4 *trans* to Cl), 7.24 (t, 1H, 5-C_6H_4 *trans* to CH_2Ph), 7.82 (d, 1H, 6-C_6H_4 *trans* to Cl), 8.55 (d, 1H, 6-C_6H_4 *trans* to CH_2Ph). ^{13}C NMR (100 MHz, C_6D_6, 35 °C): δ 11.8 (q, $^1J_{C-H}$ = 128 Hz, C_5Me_5), 19.4 (q, $^1J_{C-H}$ = 116 Hz, CH_3), 19.4 (q, $^1J_{C-H}$ = 116 Hz, CH_3), 61.6 (t, $^1J_{C-H}$ = 122 Hz, CH_2-Ph), 109.2 (d, $^1J_{C-H}$ = 185 Hz, N=CH−), 111.4 (d, $^1J_{C-H}$ = 180 Hz, N=CH−), 120.0 (s, C_5Me_5), 122.2 (d, $^1J_{C-H}$ = 158 Hz, *p*-C_6H_5), 125.3, 125.6, 125.6, 125.7, 126.0, and 126.1 (d, $^1J_{C-H}$ = 156−160 Hz, 3-, 5-, and 6-C_6H_4), 126.9 (d, $^1J_{C-H}$ = 157 Hz, *m*-C_6H_5), 128.5 (d, $^1J_{C-H}$ = 167 Hz, *o*-C_6H_5), 130.4 (d, $^1J_{C-H}$ = 154 Hz, 4-C_6H_4), 131.1 (d, $^1J_{C-H}$ = 156 Hz, 4-C_6H_4), 134.0 (s, 2-C_6H_4), 134.2 (s, 2-C_6H_4), 149.2 (s, 1-C_6H_4), 149.9 (s, 1-C_6H_4), 153.9 (s, *ipso*-C_6H_5). IR (KBr): ν(CN)/cm^{-1} 1482 (s), 1461 (s). Anal. Calcd for $C_{33}H_{38}ClN_2Ta$: C, 58.37; H, 5.64; N, 4.13. Found: C, 58.69; H, 5.70; N, 4.13.

Preparation of M(=CHPh)Cp*(*p*-MeOC_6H_4-dad) (17, M = Ta; 18, M = Nb). Complex **12** (11 mg, 0.014 mmol) was dissolved in 0.58 mL of C_6D_6 in a 5 mm NMR tube. The solution was heated to 35 °C for 12 h, and ^{1}H NMR was measured. The spectrum showed the formation of **17** along with the signal due to toluene (protons of methyl group: δ 2.16). ^{1}H NMR (400 MHz, C_6D_6, 35 °C): δ 1.91 (s, 15H, C_5-Me_5), 3.32 (s, 6H, OCH_3), 5.84 (s, 2H, N=CH−), 6.7−7.2 (13H, aromatic protons), 7.95 (s, 1H, Ta=C*H*Ph). ^{13}C NMR (100 MHz, C_6D_6, 35 °C): δ 11.1 (q, $^1J_{C-H}$ = 127 Hz, C_5Me_5), 55.1 (q, $^1J_{C-H}$ = 143 Hz, CH_3), 102.1 (d, $^1J_{C-H}$ = 172 Hz, N=CH−), 114.2 (s, C_5Me_5), 114.8 (d, $^1J_{C-H}$ = 158 Hz, *m*-C_6H_4), 120.5 (d, $^1J_{C-H}$ = 158 Hz, *o*-C_6H_4), 122.8 (d, $^1J_{C-H}$ = 158 Hz, *p*-C_6H_5), 127.4 (d, $^1J_{C-H}$ = 155 Hz, *m*-C_6H_5), 129.1 (d, $^1J_{C-H}$ = 157 Hz, *o*-C_6H_5), 141.6 (s, *ipso*-C_6H_4), 147.3 (s, *ipso*-C_6H_5), 156.2 (s, *p*-C_6H_4), 222.6 (d, $^1J_{C-H}$ = 124 Hz, Ta=*C*HPh).

18: ^{1}H NMR (400 MHz, C_6D_6, 35 °C) δ 1.88 (s, 15H, C_5Me_5), 3.37 (s, 6H, OCH_3), 6.06 (s, 2H, N=CH−), 6.7−7.2 (13H, aromatic protons), 8.49 (s, 1H, Nb=C*H*Ph); there are some impurities due to the reduction of **13**.

Preparation of Ta(=CHPh)Cp*(Cy-dad) (19). Complex **14** (10 mg, 0.016 mmol) was dissolved in 0.58 mL of C_6D_6 in a 5 mm NMR tube. The solution was heated to 40 °C for 24 h, and ^{1}H NMR was measured. The spectrum showed a signal of toluene which was formed by α-hydrogen elimination (protons of methyl group: δ 2.16). ^{1}H NMR (400 MHz, C_6D_6, 35 °C): δ 0.9−2.1 (m, 20H, Cy), 1.93 (s, 15H, C_5Me_5), 3.33 (m, 2H, Cy), 5.14 (s, 2H, N=CH−), 6.68 (t, $^3J_{H-H}$ = 7.3 Hz, 1H, *p*-C_6H_5), 6.90 (d, $^3J_{H-H}$ = 7.3 Hz, 2H, *o*-C_6H_5), 7.37 (t, $^3J_{H-H}$ = 7.3 Hz, 2H, *m*-C_6H_5), 7.95 (s, 1H, Ta=C*H*Ph). ^{13}C NMR (100 MHz, C_6D_6, 35 °C): δ 11.3 (q, $^1J_{C-H}$ = 127 Hz, C_5Me_5), 26.2 (t, $^1J_{C-H}$ = 124 Hz, Cy), 26.3 (t, $^1J_{C-H}$ = 124 Hz, Cy), 26.4 (t, $^1J_{C-H}$ = 124 Hz, Cy), 34.6 (t, $^1J_{C-H}$ = 129 Hz, Cy), 38.1 (t, $^1J_{C-H}$ = 125 Hz, Cy), 62.1 (d, $^1J_{C-H}$ = 132 Hz, Cy), 100.9 (d, $^1J_{C-H}$ = 169 Hz, N=CH−), 113.0 (s, C_5Me_5), 120.4 (d, $^1J_{C-H}$ = 158 Hz, *p*-C_6H_5), 126.9 (d, $^1J_{C-H}$ = 154 Hz, *m*-C_6H_5), 129.3 (d, $^1J_{C-H}$ = 156 Hz, *o*-C_6H_5), 148.6 (s, *ipso*-C_6H_5), 222.9 (d, $^1J_{C-H}$ = 129 Hz, Ta=*C*HPh).

The formation of **19** was monitored by ^{1}H NMR spectroscopy. The decrease of **14** in toluene-d_8 was found to be first-order in the temperature range between 65 and 85; the obtained thermodynamic parameters $\Delta G^{\ddagger}$, $\Delta H^{\ddagger}$, and $\Delta S^{\ddagger}$ at 75 °C are 26.4 ± 0.3 kcal/mol, 24.5 ± 0.2 kcal/mol, and −5.4 ± 0.6 cal/(K·mol), respectively.

Preparation of TaCp*(*p*-MeOC$_6$H$_4$-dad)(1,3-butadiene) (20a). To a solution of **3a** (429 mg, 0.655 mmol) in THF (30 mL) cooled at −78 °C was added a suspension of [Mg(diene)(thf)$_2$]$_n$ (1.2 equiv, 0.786 mmol). The reaction mixture was stirred for 8 h at 25 °C, and then all volatiles were removed to dryness. The product was extracted into three portions of THF (60 mL). Concentration of the solution to ca. 5 mL gave dark red microcrystals, which were rinsed with two portions of hexane (0.5 mL), 52% yield, mp 209−212 °C (dec). ^{1}H NMR (270 MHz, C$_6$D$_6$, 35 °C): δ 0.24 (m, 2H, =CH$_2$ (*anti*)), 1.66 (s, 15H, C$_5$Me$_5$), 2.26 (m, 2H, =CH$_2$ (*syn*)), 3.48 (s, 6H, OCH$_3$), 4.93 (m, 2H, C=CH−), 6.71 (s, 2H, N=CH−), 6.91 (m, 4H, *m*-C$_6$H$_4$), 7.15 (m, 4H, *o*-C$_6$H$_4$). ^{13}C NMR (100 MHz, C$_6$D$_6$, 35 °C): δ 11.9 (q, $^1J_{C-H}$ = 127 Hz, C$_5$*Me*$_5$), 53.8 (t, $^1J_{C-H}$ = 143 Hz, =CH$_2$), 55.3 (q, $^1J_{C-H}$ = 143 Hz, OCH$_3$), 113.3 (d, $^1J_{C-H}$ = 156 Hz, *m*-C$_6$H$_4$), 116.7 (s, *C*$_5$Me$_5$), 120.5 (d, $^1J_{C-H}$ = 165 Hz, C=*C*H−), 125.3 (d, $^1J_{C-H}$ = 156 Hz, *o*-C$_6$H$_4$), 131.2 (d, $^1J_{C-H}$ = 170 Hz, N=CH−), 148.8 (s, *ipso*-C$_6$H$_4$), 156.5 (s, *p*-C$_6$H$_4$). IR (KBr): ν(CN)/cm^{-1} 1499 (s). FAB mass spectrum *m*/*z* = 639 (M$^+$). UV (toluene) λ_{max} = 409 nm (ϵ = 6.6 × 10^3) and 513 nm (ϵ = 7.7 × 10^3). Anal. Calcd for C$_{30}$H$_{37}$N$_2$O$_2$Ta: C, 56.43; H, 5.84; N, 4.39. Found: C, 56.03; H, 5.69; N, 4.31.

Complexes **20b**, **21a**, and **21b** were prepared in similar manner.

20b: 56% yield, mp 112−125 °C (dec). ^{1}H NMR (270 MHz, C$_6$D$_6$, 35 °C): δ 0.42 (m, 2H, =CH$_2$ (*anti*)), 2.34 (m, 2H, =CH$_2$ (*syn*)), 3.48 (s, 6H, OCH$_3$), 4.91 (m, 2H, C=CH−), 5.62 (s, 5H, C$_5$H$_5$), 6.75 (s, 2H, N=CH−), 6.91 (m, 4H, *m*-C$_6$H$_4$), 7.11 (m, 4H, *o*-C$_6$H$_4$). ^{13}C NMR (100 MHz, C$_6$D$_6$, 35 °C): δ 49.3 (t, $^1J_{C-H}$ = 149 Hz, =CH$_2$), 55.2 (q, $^1J_{C-H}$ = 143 Hz, OCH$_3$), 105.5 (d, $^1J_{C-H}$ = 176 Hz, C$_5$H$_5$), 114.0 (d, $^1J_{C-H}$ = 160 Hz, *m*-C$_6$H$_4$), 120.7 (d, $^1J_{C-H}$ = 163 Hz, C=*C*H−), 123.2 (d, $^1J_{C-H}$ = 152 Hz, *o*-C$_6$H$_4$), 130.3 (d, $^1J_{C-H}$ = 170 Hz, N=CH−), 149.0 (s, *ipso*-C$_6$H$_4$), 156.5 (s, *p*-C$_6$H$_4$). IR (KBr): ν(CN)/cm^{-1} 1499 (s). FAB mass spectrum *m*/*z* = 568 (M$^+$). UV (toluene) λ_{max} = 421 nm (ϵ = 3.0 × 10^3), 512 nm (ϵ = 2.9 × 10^3). Anal. Calcd for C$_{25}$H$_{27}$N$_2$O$_2$Ta: C, 52.82; H, 4.79; N, 4.93. Found: C, 52.60; H, 4.78; N, 4.95.

21a: 76% yield, mp 195−198 °C (dec). ^{1}H NMR (400 MHz, C$_6$D$_6$, 35 °C): δ 0.52 (m, 2H, =CH$_2$ (*anti*)), 1.60 (s, 15H, C$_5$Me$_5$), 2.61 (m, 2H, =CH$_2$ (*syn*)), 3.47 (s, 6H, OCH$_3$), 4.71 (m, 2H, C=CH−), 6.67 (s, 2H, N=CH−), 6.90 (m, 4H, *m*-C$_6$H$_4$), 7.19 (m, 4H, *o*-C$_6$H$_4$). ^{13}C NMR (100 MHz, C$_6$D$_6$, 35 °C): δ 12.0 (q, $^1J_{C-H}$ = 127 Hz, C$_5$*Me*$_5$), 55.2 (q, $^1J_{C-H}$ = 143 Hz, OCH$_3$), 57.4 (t, $^1J_{C-H}$ = 144 Hz, =CH$_2$), 113.4 (d, $^1J_{C-H}$ = 157 Hz, *m*-C$_6$H$_4$), 116.3 (s, *C*$_5$Me$_5$), 119.1 (d, $^1J_{C-H}$ = 159 Hz, C=*C*H−), 124.7 (d, $^1J_{C-H}$ = 157 Hz, *o*-C$_6$H$_4$), 132.4 (d, $^1J_{C-H}$ = 168 Hz, N=CH−), 149.0 (s, *ipso*-C$_6$H$_4$), 156.9 (s, *p*-C$_6$H$_4$). UV (toluene) λ_{max} = 441 nm (ϵ = 2.4 × 10^3), 546 nm (ϵ = 2.5 × 10^3). IR (KBr): ν(CN)/cm^{-1} 1503 (s). Anal. Calcd for C$_{30}$H$_{37}$N$_2$O$_2$Nb: C, 65.45; H, 6.77; N, 5.09. Found: C, 65.50; H, 6.78; N, 4.95.

21b: 48% yield, mp 87−93 °C (dec). ^{1}H NMR (270 MHz, C$_6$D$_6$, 35 °C): δ 0.76 (m, 2H, =CH$_2$ (*anti*)), 2.66 (m, 2H, =CH$_2$ (*syn*)), 3.47 (s, 6H, OCH$_3$), 4.63 (m, 2H, C=CH−), 5.60 (s, 5H, C$_5$H$_5$), 6.73 (s, 2H, N=CH−), 6.85 (m, 4H, *m*-C$_6$H$_4$), 7.17 (m, 4H, *o*-C$_6$H$_4$). ^{13}C NMR (100 MHz, C$_6$D$_6$, 35 °C): δ 52.2 (t, $^1J_{C-H}$ = 151 Hz, =CH$_2$), 55.2 (q, $^1J_{C-H}$ = 143 Hz, OCH$_3$), 105.1 (d, $^1J_{C-H}$ = 174 Hz, C$_5$H$_5$), 114.0 (d, $^1J_{C-H}$ = 158 Hz, *m*-C$_6$H$_4$), 119.3 (d, $^1J_{C-H}$ = 164 Hz, C=*C*H−), 122.7 (d, $^1J_{C-H}$ = 157 Hz, *o*-C$_6$H$_4$), 131.6 (d, $^1J_{C-H}$ = 169 Hz, N=CH−), 149.3 (s, *ipso*-C$_6$H$_4$), 156.9 (s, *p*-C$_6$H$_4$). UV (toluene) λ_{max} = 456 nm (ϵ = 1.2 × 10^3), 542 nm (ϵ = 1.2 × 10^3). IR (KBr): ν(CN)/cm^{-1} 1498 (s). Anal. Calcd for C$_{25}$H$_{27}$N$_2$O$_2$Nb: C, 62.50; H, 5.66; N, 5.83. Found: C, 62.21; H, 6.04; N, 6.10.

Preparation of TaCp*(*p*-Tol-dad)(1,3-butadiene) (22). To a solution of **5** (418 mg, 0.671 mmol) in THF (30 mL) cooled at −78 °C was added a suspension of [Mg(diene)(thf)$_2$]$_n$ (1.2 equiv, 0.805 mmol). The reaction mixture was stirred for 5 h at 25 °C, and then all volatiles were removed to dryness. The product was extracted into three portions of hexane (60 mL). Concentration of the solution to ca. 1 mL gave dark red microcrystals, which were rinsed with two portions of hexane (0.5 mL), 60% yield, mp 180−187 °C (dec). ^{1}H NMR (400 MHz, C$_6$D$_6$, 35 °C): δ 0.24 (m, 2H, =CH$_2$ (*anti*)), 1.67 (s, 15H, C$_5$Me$_5$), 2.23 (m, 2H, =CH$_2$ (*syn*)), 2.32 (s, 6H, CH$_3$), 4.93 (m, 2H, C=CH−), 6.73 (s, 2H, N=CH−), 7.10 (m, 4H, C$_6$H$_4$), 7.14 (m, 4H, C$_6$H$_4$). ^{13}C NMR (100 MHz, C$_6$D$_6$, 35 °C): δ 11.9 (q, $^1J_{C-H}$ = 127 Hz, C$_5$*Me*$_5$), 20.9 (q, $^1J_{C-H}$ = 127 Hz, CH$_3$), 54.2 (t, $^1J_{C-H}$ = 144 Hz, =CH$_2$), 117.0 (s, *C*$_5$Me$_5$), 120.6 (d, $^1J_{C-H}$ = 165 Hz, C=*C*H−), 124.4 (d, $^1J_{C-H}$ = 158 Hz, *o*-C$_6$H$_4$), 129.3 (d, $^1J_{C-H}$ = 158 Hz, *m*-C$_6$H$_4$), 131.1 (d, $^1J_{C-H}$ = 170 Hz, N=CH−), 132.0 (s, *p*-C$_6$H$_4$), 152.8 (s, *ipso*-C$_6$H$_4$). FAB mass spectrum *m*/*z* = 606 (M$^+$), 552 (M − C$_4$H$_6$)$^+$. UV (toluene) λ_{max} = 402 nm (ϵ = 3.6 × 10^3) and 517 nm (ϵ = 3.3 × 10^3). IR (KBr): ν(CN)/cm^{-1} 1502 (s). Anal. Calcd for C$_{30}$H$_{37}$N$_2$Ta: C, 59.40; H, 6.15; N, 4.62. Found: C, 59.60; H, 6.30; N, 4.49.

Preparation of TaCp*(Cy-dad)(1,3-butadiene) (23). To a solution of **7** (232 mg, 0.381 mmol) in THF (20 mL) cooled −78 °C was added a suspension of [Mg(diene)(thf)$_2$]$_n$ (1.0 equiv, 0.381 mmol). The reaction mixture was stirred for 1 h at 25 °C. Then the mixture was evaporated to dryness, and the product was extracted into two portions of THF (60 mL). Concentration of the solution to ca. 1 mL gave **23** as deep purple microcrystals, 59% yield, mp 207−210 °C (dec). ^{1}H NMR (400 MHz, C$_6$D$_6$, 35 °C): δ −0.27 (m, 2H, =CH$_2$ (*anti*)), 1.15, 1.29, 1.38, 1.58, 1.63, 1.78, 1.87, and 2.01 (m, 22H, cyclohexyl protons), 1.94 (s, 15H, C$_5$Me$_5$), 3.41 (m, 2H, =CH$_2$ (*syn*)), 4.61 (m, 2H, C=CH−), 6.68 (s, 2H, N=CH−). ^{13}C NMR (100 MHz, C$_6$D$_6$, 35 °C): δ 11.4 (q, $^1J_{C-H}$ = 127 Hz, C$_5$*Me*$_5$), 26.0 (t, $^1J_{C-H}$ = 121 Hz, cyclohexyl carbons), 27.0 (t, $^1J_{C-H}$ = 123 Hz, cyclohexyl carbons), 27.7 (t, $^1J_{C-H}$ = 126 Hz, cyclohexyl carbons), 32.4 (t, $^1J_{C-H}$ = 124 Hz, cyclohexyl carbons), 38.2 (t, $^1J_{C-H}$ = 127 Hz, cyclohexyl carbons), 46.9 (t, $^1J_{C-H}$ = 144 Hz, =CH$_2$), 65.1 (d, $^1J_{C-H}$ = 129 Hz, cyclohexyl carbons), 114.6 (s, *C*$_5$Me$_5$), 118.2 (d, $^1J_{C-H}$ = 161.1 Hz, C=*C*H−), 126.4 (d, $^1J_{C-H}$ = 165 Hz, N=CH−). UV (toluene) λ_{max} = 529 nm (ϵ = 4.1 × 10^3). IR (KBr): ν(CN)/cm^{-1} 1447 (s). Anal. Calcd for C$_{28}$H$_{45}$N$_2$Ta: C, 56.94; H, 7.68; N, 4.74. Found: C, 57.27; H, 7.77; N, 4.65.

Crystallographic Data Collections and Structure Determination of 3a, 4a, 5, 7, 10, 14, 16, and 23. Data Collection. The crystals of **3a**, **4a**, **5**, **7**, **10**, **14**, **16**, and **23** suitable for X-ray diffraction studies were sealed in glass capillaries under an argon atmosphere, and then a crystal of each complex was mounted on a Rigaku AFC-7R four-circle diffractometer for data collection using Mo Kα (graphite-monochromated, λ = 0.710 69) radiation. Relevant crystal and data statistics are summarized in Table 4. The unit cell parameters and the orientation matrix at 23 °C were determined by a least-squares fit to 2θ values of 25 strong higher reflections for all complexes. Three standard reflections were chosen and monitored every 150 reflections. For all of the complexes except for **10**, an empirical absorption correction was applied on the basis of azimuthal scans. The data for all complexes were corrected for Lorentz and polarization effects.

Structural Determinations and Refinements. The structures of complexes **5**, **14**, **16**, and **23** were solved by a direct method (SHELXS 86)[54] and refined by the full-matrix least-squares method. The structures of complexes **3a**, **4a**, **7**, and **10** were solved by a heavy-atom Patterson method (PATTY 92)[55] and refined by the full-matrix least-squares method. Measured nonequivalent reflections were used for the structure determination. In the subsequent refinement the function $\sum\omega(|F_o| - |F_c|)^2$ was minimized, where $|F_o|$ and $|F_c|$ are the

(54) Sheldrick, G. M. In *Crystallographic Computing 3*; Sheldrick, G. M., Krüger, C., Goddard, R., Eds.; Oxford University Press: Oxford, 1985; p 179.

(55) Beurskens, P. T.; Admiraal, G.; Beurskens, G.; Boeman, W. P.; Garcia-Granda, S.; Gould, R. O.; Smits, J. M. M.; Smykalla, C. *The DIRDIF program system*, Technical Report of the Crystallography Laboratory; University of Nijmegen, The Netherland, 1992.

Table 4. Crystal Data and Data Collection Parameters of 3a, 4a, 5, 7, 10, 14, 16, and 23

	3a	**4a**	**5**	**7**
formula	$C_{26}H_{31}Cl_2N_2O_2Ta$	$C_{26}H_{31}Cl_2N_2O_2Nb$	$C_{26}H_{31}Cl_2N_2Ta$	$C_{24}H_{39}N_2Cl_2Ta$
fw	655.40	567.36	623.40	607.44
cryst syst	monoclinic	monoclinic	monoclinic	monoclinic
space group	*C*2/*c* (No. 15)	*P*2$_1$/*c* (No. 14)	*P*2$_1$/*n* (No. 14)	*P*2$_1$/*c* (No. 14)
a, Å	24.97(1)	9.474(3)	15.354(5)	12.447(2)
b, Å	9.882(6)	9.102(4)	22.258(6)	13.403(4)
c, Å	23.434(7)	30.182(7)	15.929(5)	16.915(3)
α, deg				
β, deg	102.10(3)	92.21(2)	111.70(2)	91.09(1)
γ, deg				
V, Å^3	5653(4)	2600(1)	5058(2)	2821.5(10)
Z	8	4	8	4
D_{calcd}, g/cm^{-3}	1.540	1.449	1.637	1.430
F(000)	2592.00	1168.00	2464.00	1216.00
μ [Mo Kα], cm^{-1}	40.95	6.93	45.66	40.90
T, °C	23	23	23	23
cryst size, mm	0.2 × 0.2 × 0.2	0.5 × 0.2 × 0.2	0.3 × 0.2 × 0.2	0.5 × 0.3 × 0.2
scan type	*ω*−2*θ*	*ω*	*ω*−2*θ*	*ω*−2*θ*
scan speed, deg/min	16	32	16	16
scan width, deg	1.00 + 0.30 tan *θ*	0.73 + 0.30 tan *θ*	0.89 + 0.30 tan *θ*	1.21 + 0.30 tan *θ*
$2\theta_{min}$, $2\theta_{max}$, deg	6.0, 55.0	5.0, 55.0	5.0, 55.0	5.0, 55.0
unique data (R_{int})	6855 (0.104)	6350 (0.039)	11 923 (0.055)	6738 (0.025)
no. of observations	6468	5964	11 612	6399
no. of variables	299	298	560	262
R1, wR2 (all data)	0.228, 0.178	0.091, 0.091	0.082, 0.082	0.077, 0.112
R, R_w	0.065, 0.080 ($I > 3.0\sigma(I)$)	0.037, 0.038 ($I > 3.0\sigma(I)$)	0.040, 0.041 ($I > 3.0\sigma(I)$)	0.038, 0.046 ($I > 3.0\sigma(I)$)
GOF on F^2	1.54	1.07	1.41	1.43
Δ, e Å^{-3}	3.89, −3.75	0.98, −1.44	2.17, −2.01	2.15, −1.33

	10	**14**	**16**	**23**
formula	$C_{28}H_{37}N_2O_2Ta$	$C_{38}H_{53}N_2Ta$	$C_{33}H_{38}ClN_2Ta$	$C_{28}H_{45}N_2Ta$
fw	614.56	718.80	679.08	590.62
cryst syst	triclinic	monoclinic	monoclinic	monoclinic
space group	*P*$\bar{1}$ (No. 2)	*P*2$_1$/*c* (No. 14)	*P*2$_1$/*n* (No. 14)	*P*2$_1$/*c* (No. 14)
a, Å	10.056(2)	12.093(4)	9.751(3)	18.271(6)
b, Å	16.387(4)	16.015(6)	22.491(4)	16.161(6)
c, Å	8.386(3)	16.873(7)	15.180(4)	26.449(10)
α, deg	102.89(3)			
β, deg	95.32(2)	95.79(3)	107.15(2)	91.78(3)
γ, deg	100.27(2)			
V, Å^3	1312.7(7)	3251(1)	3181(1)	7805(3)
Z	2	4	4	12
D_{calcd}, g/cm^{-3}	1.555	1.468	1.418	1.508
F(000)	616.00	1472.00	1360.00	3600.00
μ [Mo Kα], cm^{-1}	42.06	34.04	35.56	42.35
T, °C	23	23	23	23
cryst size, mm	0.3 × 0.2 × 0.1	0.5 × 0.3 × 0.2	0.4 × 0.2 × 0.1	0.2 × 0.2 × 0.1
scan type	*ω*−2*θ*	*ω*−2*θ*	*ω*−2*θ*	*ω*
scan speed, deg/min	32	16	16	16
scan width, deg	1.94 + 0.30 tan *θ*	0.94 + 0.30 tan *θ*	1.21 + 0.30 tan *θ*	1.05 + 0.30 tan *θ*
$2\theta_{min}$, $2\theta_{max}$, deg	5.0, 55.0	5.0, 55.0	5.0, 55.0	5.0, 55.9
unique data (R_{int})	5193 (0.038)	6795 (0.041)	7501 (0.032)	18 569 (0.075)
no. of observations	5125	6547	7241	17 913
no. of variables	298	371	334	839
R1, wR2 (all data)	0.057, 0.065	0.084, 0.084	0.085, 0.086	0.132, 0.133
R, R_w	0.035, 0.036 ($I > 1.5\sigma(I)$)	0.037, 0.038 ($I > 3.0\sigma(I)$)	0.040, 0.041 ($I > 3.0\sigma(I)$)	0.048, 0.049 ($I > 1.5\sigma(I)$)
GOF on F^2	1.99	1.20	1.75	1.08
Δ, e Å^{-3}	1.30, −1.52	1.60, −1.64	2.37, −1.49	3.43, −3.03

observed and calculated structure factor amplitudes, respectively. The agreement indices are defined as $R1 = \sum(||F_o| - |F_c||)/\sum|F_o|$ and $wR2 = [\sum\omega(F_o^2 - F_c^2)^2/\sum(\omega F_o^4)]^{1/2}$. The positions of all non-hydrogen atoms for all complexes were found from a difference Fourier electron density map and refined anisotropically. All hydrogen atoms were placed in calculated positions (C−H = 0.95 Å) and kept fixed. All calculations were performed using the TEXSAN crystallographic software package, and illustrations were drawn with ORTEP. Refinements by using the agreement index w*R*2 were also applied to complexes **3b** and **20a**, although these have already been refined and reported.[12]

Acknowledgment. This work was financially supported by a Grant-in-Aid for Scientific Research on Priority Area (No. 283, "Innovative Synthetic Reactions") from the Ministry of Education, Science and Culture, Japanese government. K.M. appreciates the partial financial support from the Yamada Science Foundation. Y.M. is a research fellow of the Japan Society for the Promotion of Science, 1998−2000.

Supporting Information Available: Final positional parameters, final thermal parameters, bond distances, angles, and best planes for all complexes crystallographically characterized; ^{1}H NMR spectra of complexes **9**, **17**, **18**, and **19**; UV spectra of **20a** and **23**. This material is available free of charge via the Internet at http://pubs.acs.org.

OM981003B